A Section 508–conformant HTML version of this article is available at https://doi.org/10.1289/EHP8171.

Sex-Specific Effects of Prenatal and Early Life Inorganic and Methylated Arsenic Exposure on Atherosclerotic Plaque Development and Composition in Adult ApoE$^{-/-}$ Mice

Luis Fernando Negro Silva,[1] Kiran Makhani,[1*] Maryse Lemaire,[1] Catherine A. Lemarié,[1,2,3] Dany Plourde,[1] Alicia M. Bolt,[1] Christopher Chiavatti,[1] D. Scott Bohle,[4] Stéphanie Lehoux,[1] Mark S. Goldberg,[5,6,7] and Koren K. Mann[1]*

[1]Lady Davis Institute for Medical Research, McGill University, Montreal, Quebec, Canada
[2]EA3878, European University of Occidental Brittany, Brest, France
[3]UMR 1078, Institut national de la santé et de la recherché médicale, Brest, France
[4]Department of Chemistry, McGill University, Montreal, Quebec, Canada
[5]Department of Medicine, McGill University, Montreal, Quebec, Canada
[6]Department of Epidemiology, Biostatistics, and Occupational Health, McGill University, Montreal, Quebec, Canada
[7]Division of Clinical Epidemiology, Research Institute of the McGill University Health Centre, Montreal, Quebec, Canada

Background: Epidemiologic studies indicate that early life arsenic exposures are linked to an increased risk of cardiovascular diseases. Different oxidation and methylation states of arsenic exist in the environment and are formed *in vivo* via the action of arsenic (+3 oxidation state) methyltransferase (As3MT). Methylated arsenicals are pro-atherogenic postnatally, but pre- and perinatal effects are unclear. This is particularly important because methylated arsenicals are known to cross the placenta.

Objectives: We tested the effects of early life exposure to inorganic and methylated arsenicals on atherosclerotic plaque formation and its composition in apolipoprotein E knock-out (apoE$^{-/-}$) mice and evaluated whether apoE$^{-/-}$ mice lacking As3MT expression were susceptible to this effect.

Methods: We exposed apoE$^{-/-}$ or apoE$^{-/-}$/As3MT$^{-/-}$ mice to 200 ppb inorganic or methylated arsenic in the drinking water from conception to weaning and assessed atherosclerotic plaques in the offspring at 18 wk of age. Mixed regression models were used to estimate the mean difference in each outcome relative to controls, adjusting for sex and including a random effects term to account for within-litter clustering.

Results: Early life exposure to inorganic arsenic, and more profoundly methylated arsenicals, resulted in significantly larger plaques in the aortic arch and sinus in both sexes. Lipid levels in these plaques were higher without a substantial difference in macrophage numbers. Smooth muscle cell content was not altered, but collagen content was lower. Importantly, there were sex-specific differences in these observations, where males had higher lipids and lower collagen in the plaque, but females did not. In mice lacking As3MT, arsenic did not alter the plaque size, although the size was highly variable. In addition, control apoE$^{-/-}$/As3MT$^{-/-}$ mice had significantly larger plaque size compared with control apoE$^{-/-}$.

Conclusion: This study shows that early life exposure to inorganic and methylated arsenicals is pro-atherogenic with sex-specific differences in plaque composition and a potential role for As3MT in mice. https://doi.org/10.1289/EHP8171

Introduction

Arsenic is a toxicant naturally found in soil, water, and air. (Mandal and Suzuki 2002; Nordstrom 2002). The World Health Organization (WHO) has set a maximum contaminant level of arsenic at 10 ppb for municipal drinking water (WHO 2008), but millions of people worldwide are exposed to elevated levels of arsenic (Nordstrom 2002). Arsenic increases the risk of several diseases, from cancer to cardiovascular disease (CVD) (Chen et al. 2013b; James et al. 2015; Jiang et al. 2015; Kuo et al. 2017; Mateen et al. 2017; Moon et al. 2017; Roh et al. 2017; Smith et al. 2018). It has been linked epidemiologically to increased risk for atherosclerosis, the gradual occlusion of large arteries with fibrofatty plaques (Hsieh et al. 2011; Wang et al. 2010), which, in turn, increases the risk of mortality due to heart attack and stroke. However, we do not understand who is at risk for developing atherosclerosis following arsenic exposure.

Several studies have indicated that pregnancy is an important window for arsenic exposure (Young et al. 2018). *In utero* exposure to arsenic has been associated with effects in children, including decreased birth weight, potentially by decreasing gestational age and/or maternal weight gain (Kile et al. 2016; Wang et al. 2018). A number of epidemiologic studies have suggested that *in utero* arsenic exposure is also associated with several adverse health effects later in life, such as lung (Steinmaus et al. 2016) and bladder tumors (Smith et al. 2012; Yuan et al. 2007), diabetes (Navas-Acien et al. 2019), and coronary heart disease (Roseboom et al. 2000). Limited data have linked early life arsenic exposures to CVD. In a cross-sectional study of children in Mexico, increased carotid intima thickness, a marker for early atherosclerosis, was found to be associated with total urinary arsenic (Osorio-Yáñez et al. 2013). Although the contribution of *in utero* exposure could not be defined, most of the mothers lived in the same region throughout pregnancy. In a Bangladeshi cohort, arsenic exposure was associated with a greater risk of mortality from cancer or CVD in children, albeit in a sample population with a very small death rate (Rahman et al. 2013). Thus, it is unclear whether exposure to arsenic during gestation leads to increased risk of atherosclerosis in humans.

Arsenic is metabolized by a series of oxidative methylation reactions catalyzed by the enzyme arsenic (III) methyltransferase (As3MT) (Thomas 2007). The biotransformation process is a conserved mechanism that produces methylated intermediate compounds and has historically been considered a detoxification process. However, this concept has been challenged because some of the intermediate compounds of arsenic biomethylation, particularly the methylated metabolites containing trivalent

*These authors contributed equally to this work.

Address correspondence to Koren K. Mann, Lady Davis Institute for Medical Research, McGill University, 3755 Cote Ste Catherine Rd., Montreal, QC H3T 1E2 Canada. Telephone (514) 340-8222 ext. 22760. Email: koren.mann@mcgill.ca

Supplemental Material is available online (https://doi.org/10.1289/EHP8171).

The authors declare they have no actual or potential competing financial interests.

Received 26 August 2020; Revised 26 February 2021; Accepted 19 March 2021; Published 17 May 2021.

Note to readers with disabilities: *EHP* strives to ensure that all journal content is accessible to all readers. However, some figures and Supplemental Material published in *EHP* articles may not conform to 508 standards due to the complexity of the information being presented. If you need assistance accessing journal content, please contact ehponline@niehs.nih.gov. Our staff will work with you to assess and meet your accessibility needs within 3 working days.

arsenic, were considered more toxic than the inorganic form (Stýblo et al. 2002). For example, we have shown that in mice, in addition to inorganic arsenic, methylated forms are pro-atherogenic (Negro Silva et al. 2017). Interestingly, we also showed that arsenic-enhanced plaque formation was dependent upon As3MT expression (Negro Silva et al. 2017). This suggests that arsenic methylation is essential for the atherogenic properties of arsenic after postnatal exposure in mice. Based on the urinary profile of arsenic metabolites in epidemiologic studies, several factors may contribute to the efficiency of the biotransformation reaction, such as nutritional status (Hall et al. 2007; Howe et al. 2014; Pilsner et al. 2009), genetic background (Meza et al. 2007; Schläwicke Engström et al. 2007), gender (Lindberg et al. 2008; Vahter et al. 2002), and pregnancy (Concha et al. 1998). Indeed, pregnant women have a more efficient methylation process (Concha et al. 1998; Hall et al. 2007). Arsenic and methylated intermediates pass through the placenta, and thus the fetus has been shown to be exposed to similar concentrations of arsenic as the mother (Concha et al. 1998; Hall et al. 2007). Pregnancy and development are considered susceptible periods of exposure to toxicants (Farzan et al. 2013), but the sequela from exposure to arsenic during gestation have not been well defined.

Animal experiments have provided mechanistic insight into the underlying mechanisms of arsenic-enhanced atherosclerosis. We previously showed that postnatal exposure to low (10–50 ppb)-to-moderate (100–200 ppb) concentrations of arsenic as sodium arsenite ($NaAsO_2$) (Lemaire et al. 2011; Makhani et al. 2018) or methylated arsenicals (Negro Silva et al. 2017) resulted in larger atherosclerotic plaques in 18-wk-old male apoE$^{-/-}$ mice. Our data also indicated that arsenic trioxide enhanced lipid accumulation in macrophages (Padovani et al. 2010) and increased the attachment of macrophages to the arterial endothelial cell layer *in vitro* (Lemaire et al. 2015). Furthermore, an *in utero* exposure to $NaAsO_2$ also increased plaque formation in apoE$^{-/-}$ mice (Srivastava et al. 2007). Microarray analysis showed that preprograming of oxidative stress and inflammatory response pathways during early life was associated with enhanced development of atherosclerosis later in life (States et al. 2012). Lipids, stress, and inflammatory pathways, which may contribute to plaque formation, were also up-regulated after arsenic exposure (as $NaAsO_2$) at high concentrations via drinking water (45 ppm/45,000 ppb) (States et al. 2012). However, it is unknown whether prenatal exposure to low-to-moderate arsenic concentrations are pro-atherogenic. In addition, the pro-atherogenic potential of methylated arsenicals and the impact of biotransformation remain to be elucidated.

Thus, we asked whether pre- and perinatal exposure to 200 ppb inorganic or methylated arsenicals would result in greater atherosclerotic plaques when measured later in life in an apoE$^{-/-}$ mouse model. Furthermore, we used our model of apoE$^{-/-}$ mice that also lack As3MT expression to determine whether arsenic-enhanced atherosclerosis following gestational exposure was dependent upon As3MT.

Material and Methods

Mice and Exposure Protocol

B6.129P2-*ApoE*^{tm1Unc}/J (apoE$^{-/-}$) mice were obtained from the Jackson Laboratory. *As3MT*$^{-/-}$ mice (C57BL/6 background) were kindly provided by D. Thomas (U.S. Environmental Protection Agency, Research Triangle Park, NC) and used to create apoE$^{-/-}$/As3MT$^{-/-}$ double-knockout (DKO) mice in our facility (Negro Silva et al. 2017). Purchased mice were acclimatized to housing conditions under a 12-h light/12-h dark cycle for at least 2 wk before experiments. All mice were fed *ad libitum*. Female mice were fed AIN-76A purified diet (Harlan Laboratories Inc.) containing 5% fat (by weight) with no cholesterol 1 wk prior to mating, and then parents and offspring were maintained on AIN-76A. The experimental protocol was approved by the McGill Animal Care Committee, and animals were handled in accordance with institutional guidelines. The McGill Animal Care Committee is certified by the Canadian Council on Animal Care.

Both apoE$^{-/-}$ and apoE$^{-/-}$As3MT$^{-/-}$ mice were assigned randomly by sex to mating pairs ($n \geq 4$ pairs per experimental group). ApoE$^{-/-}$ mating pairs were exposed to either tap water or tap water containing 200 ppb arsenic in the form of *m*-$NaAsO_2$ (0.35 mg/L $NaAsO_2$; Sigma-Aldrich), disodium methyl arsonate hexahydrate (MMA^V; 0.78 mg/L; Chem Service), cacodylic acid (DMA^V; 0.43 mg/L; Sigma-Aldrich) or monomethylarsonous acid [MMA^{III}; 0.37 mg/L]. This is a concentration at which we have observed maximal pro-atherogenic effects postnatally (Lemaire et al. 2011; Makhani et al. 2018). This level of arsenic has been found in the drinking water in highly contaminated areas of Bangladesh (BGS 2000), Argentina (Pérez-Carrera and Fernández Cirelli 2010; Concha et al. 1998), and the United States (Neilsen et al. 2010). The synthesis of MMA^{III} is described in the next section. Moreover, apoE$^{-/-}$/As3MT$^{-/-}$ mice were exposed to either tap water or tap water containing 200 ppb arsenic in the form of *m*-$NaAsO_2$ (0.35 mg/L $NaAsO_2$; Sigma-Aldrich). Solutions containing arsenic were prepared fresh from the powder every 2 to 3 days to minimize oxidation and hydrolytic demethylation. After confirmation of pregnancy via weight gain and vaginal plug observations in female mice, male mice were removed from the cage and pregnant females were housed separately until weaning. Exposure was from mating until 3 wk after birth. ApoE$^{-/-}$ dams are sensitive to stress and environmental changes, thus to assure care of the pups, we waited until 3 wk post-birth to change to tap water. At weaning (Wk 4), both control and exposed apoE$^{-/-}$ or DKO pups were maintained for an additional 14 wk on tap water. At 18 wk of age, adult male and female offspring were euthanized by carbon dioxide asphyxiation/cervical dislocation, and subsequently, heart and aortae were collected, rinsed in phosphate-buffered saline (PBS), and fixed in 4% paraformaldehyde solution.

Synthesis of MMA^{III}

Synthesis of MMA^{III} was performed as/based on a previous publication (Cullen et al. 1989). The first step in the synthesis of MMA^{III} was to prepare methylarsine oxide [$(MeAsO)_4$] by dissolving 5.5 g of methylarsenate (MAs^V) acid sodium salt, ($CH_3AsO_3Na_2$) in 50 mL of water (H_2O), Dissolution of the initial salt was promoted by gradual heating of the solution. Once dissolved, the solution was treated with sulfur dioxide (SO_2), which was bubbled through the solution. The solution quickly becomes clear (suggesting acid sensitivity), then light yellow after another 2 min. After saturating with SO_2, the solution was quickly boiled for 2 min, then cooled for 15 min. Neutralization with sodium carbonate turned the solution from light yellow to clear. The solvent was removed and $(MeAsO)_4$ was extracted with benzene. Removing the benzene *in vacuo* resulted in 2.4 g of a white solid (70% yield).

Instant hydrolysis of this tetrameric methylarsenic oxide by dissolution in water leads to stoichiometric formation of $MeAs(OH)_2$. For example, when 0.015 g $(MeAsO)_4$ was dissolved in 1 mL water, a uniform colorless solution formed of [$MeAs(OH)_2$] in a 0.14 M concentration. When deuterium oxide (D_2O) is used in place of water, this solution has only one peak at 1.36 ppm in the ^1H nuclear magnetic resonance spectrum at 25°C, which corresponds to the methyl signal in the hydrolyzed species $MeAs(OD)_2$, as reported previously (Petrick et al. 2001).

Plasma analyses. Blood (0.6 mL) was collected by cardiac puncture and plasma was obtained using collection tubes (ethylenediaminetetraacetic acid BD Vacutainer SST). Cholesterol,

high- (HDL) and low-density (LDL) lipoproteins, triglycerides, and liver enzymes [aspartate aminotransferase (AST) and alanine aminotransferase (ALT)] were assessed by the Comparative Medicine and Animal Resources Center (CMARC at McGill University, Canada; Tables S1 and S2). The following products were used by CMARC: VITROS CHOL (Ortho-Clinical Diagnostics; 1669829) for cholesterol, VITROS dHDL (Ortho-Clinical Diagnostics; 6802469) for HDL, VITROS TRIG (Ortho-Clinical Diagnostics 8,329,930) for triglycerides, VITROS AST (Ortho-Clinical Diagnostics; 8433815) for AST, and VITROS ALT (Ortho-Clinical Diagnostics; 1655281) for ALT, as per the manufacturer's protocol. These slides employed enzyme-based methods for substrate detection followed by reflectance spectrophotometry for quantification. The quantity of LDL was calculated from HDL using the Friedwald formula.

Atherosclerotic lesion characterization. The characterization of the atherosclerotic lesions was performed as previously described (Lemaire et al. 2014, 2011; Makhani et al. 2018; Negro Silva et al. 2017). Briefly, the fixed aorta was rinsed with ultra-pure water, then cut longitudinally and stained *en face* with oil red O (Electronic Microscopy Sciences), which stains neutral triglycerides and lipids. Images were acquired using Infinity Capture software (Version 6.5.6) and a Lumenera camera. Percentage of lesion area of the aortic arch, as defined as the region from the first intercostal arteries to the ascending arch, was evaluated with ImageJ software (Schneider et al. 2012). Rinsed, fixed, and embedded frozen hearts were processed as previously described (Lemaire et al. 2011). Consecutive, 7-μm cryosections were sliced from the aortic base throughout the aortic sinus, and three to five valve sections per animal were stained with oil red O to visualize the plaque areas and analyzed for their lipid content. We considered the atherosclerotic lesions in the sinus either as lesion area in millimeters squared or as a percentage of the total sinus area. The latter calculation uses the total sinus area to normalize the data and accounts for any bias contributed by the slicing of the heart samples. The lesion area stained with oil red O (as measured by ImageJ) was divided by the total sinus area for three to five valve sections per sample. These measurements were then averaged to obtain the final plaque size (as a percentage of aortic sinus). Aortic valves were also stained and analyzed for their collagen content (type I and III) using picrosirius red (Polysciences).

In situ *immunofluorescence.* Smooth muscle cell (SMC) and macrophage content were assessed within the entire plaque area, as previously described (Lemaire et al. 2011). Briefly, slides were rinsed with PBS and blocked with 3% bovine serum albumin for 1 h. Next, they were incubated with primary antibody for 1 h at room temperature; 1:100 for monoclonal anti-α-smooth muscle cell actin [clone 1A4] (Abcam; ab7817), 1:50 for Moma-2 (Abcam; ab33451), rinsed, and incubated with fluorescently labeled secondary antibodies at room temperature for 1 h. A 1:500 dilution each of goat antimouse (Alexa 488; A11001) and a goat antirat (Alexa 488; A11006) (Invitrogen) was used to visualize α-smooth muscle cell actin and macrophages respectively. Images were acquired using Infinity Capture software and a Lumenera camera. The presence of the immunofluorescent marker from three to five sections per animal was quantified using ImageJ software (Schneider et al. 2012) and expressed as a percentage of the total lesion area to define the contribution of each component to plaque independent of plaque size.

Statistical analyses. Standard statistical analyses assume the independence of each mouse; therefore, these analyses could not be used in this *in utero* exposure study. The issue was that the mice in the same litter were more similar to each other than those from other mothers; this dependency violates the usual assumption of independence in standard statistical models (e.g., *t*-tests, regression), and thus, these correlations needed to be captured in the statistical model (Haseman and Kupper 1979; Lazic and Essioux 2013). As well, assuming independence leads to an underestimation of standard errors and consequently, biased confidence intervals (CIs) and *p*-values (Bieler and Williams 1995). The mixed-model framework (Breslow and Clayton 1993; McLean et al. 1991) accounts for these intra-litter correlations and produces appropriate inferences under certain assumptions of the model. Thus, to meet the objectives of this study, namely, to estimate the effect of arsenic on plaque size in the aortic arch and sinus and plaque contents: macrophages, lipids, collagen, and SMC, we developed simple mixed regression models in which each of the exposure groups were compared with the unexposed group for each outcome separately. The mixed-model framework accounted for the within-litter correlations by specifying that all the offspring of one dam were grouped together (a random effect was placed on the intercept for each dam). Effectively, this more complicated model is equivalent to ordinary linear regression models but accounts for the within-dam correlations, thereby providing unbiased estimates of standard errors, CIs, and *p*-values. We used the mixed-models package [nlme package in R, version 4.0.3 (R Development Core Team)] with a compound symmetry structure corresponding to a constant correlation. We routinely verified the assumptions of normality of each outcome and used standard diagnostics to ensure that the assumptions of the model were met (especially, normality of the random effects). As described previously (Caligiuri et al. 1999; Smith et al. 2010), apoE$^{-/-}$ females have larger plaques than males, independent of arsenic exposure; thus, we included sex as a covariate in our mixed-effects model. The analyses were conducted in the open-source R program, version 4.0.3 (R Development Core Team) using the lme4 function (Bates 2014a; Pinheiro and Bates 2000) and the final model was fitted using restricted maximum likelihood (REML) on the complete data set. We then formally tested for interactions between sex and exposure groups using maximum likelihood given that likelihood ratio tests cannot be used in REML. To obtain sex-specific differences, we then fitted separate models for females and males using REML. For all the statistical analyses, we considered $p < 0.05$ as statistically significant.

Table 1. Selected characteristics of the litters from control and exposed groups.

Genotype	Exposure	Litters (n)[a]	n of pups/litter	n of pups/litter (mean ± SD)	Proportion of males (%)
apoE$^{-/-}$	Control	12	3; 5; 8; 2; 2; 3; 6; 6; 6; 3; 11; 7	5.17 ± 2.73	58
	$NaAsO_2$	9	6; 9; 5; 8; 1; 9; 5; 6; 4	5.89 ± 2.57	36
	MMA^{III}	4	6; 5; 4; 7	5.50 ± 1.29	40
	MMA^{V}	5	6; 7; 8; 3; 3	5.40 ± 2.302	61
	DMA^{V}	5	3; 4; 7; 5; 6	5.00 ± 1.58	61
DKO	Control	4	5; 5; 4; 3	4.25 ± 0.96	70
	$NaAsO_2$	4	4; 7; 6; 4	5.25 ± 1.50	39

Note: DKO, double-knock out; MMA^{III}, monomethylarsonous acid; MMA^{V}, disodium methyl arsonate hexahydrate; $NaAsO_2$, sodium arsenite..
[a]These numbers represent the total number of litters exposed. However, not all litters were analyzed for all the outcomes. Outcome-specific litter numbers are presented in relevant table notes.

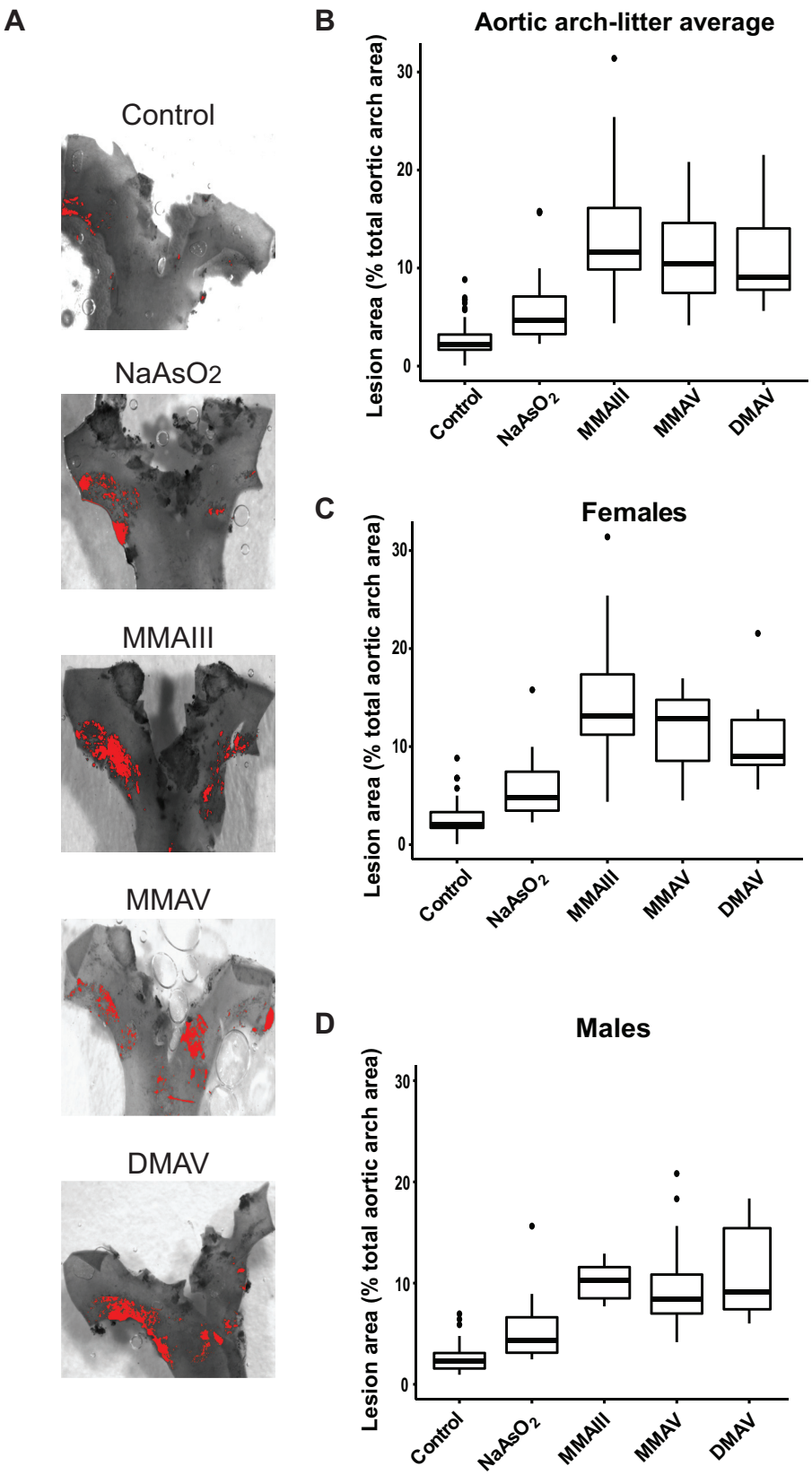

Figure 1. Differences in plaque formation in the aortic arch in adult ApoE$^{-/-}$ mice following early life arsenical exposure. ApoE$^{-/-}$ mice were exposed to 200 ppb arsenicals ($NaAsO_2$, MMA^{III}, MMA^{V}, or DMA^{V}) or maintained on tap water from conception to weaning. After weaning (4 wk), male and female pups were kept on tap water for an additional 14 wk. The percentage of the lesion area of the aortic arch was evaluated via *en face* oil red O staining. (A) Representative images. The box plots represent the distribution of unadjusted total lesion area as a percentage of total arch area, where midline, box limits, whiskers, and dots denote the median, interquartile range, minimum and maximum values, and outliers, respectively. (B) The combined data set is presented, and sex-specific data sets for (C) females and (D) are presented. The corresponding numeric data are presented in Table S4 and that adjusted by litter are presented in Tables 2 and 3. Note: DMA^{V}, cacodylic acid; MMA^{III}, monomethylarsonous acid; MMA^{V}, disodium methyl arsonate hexahydrate; $NaAsO_2$, sodium arsenite.

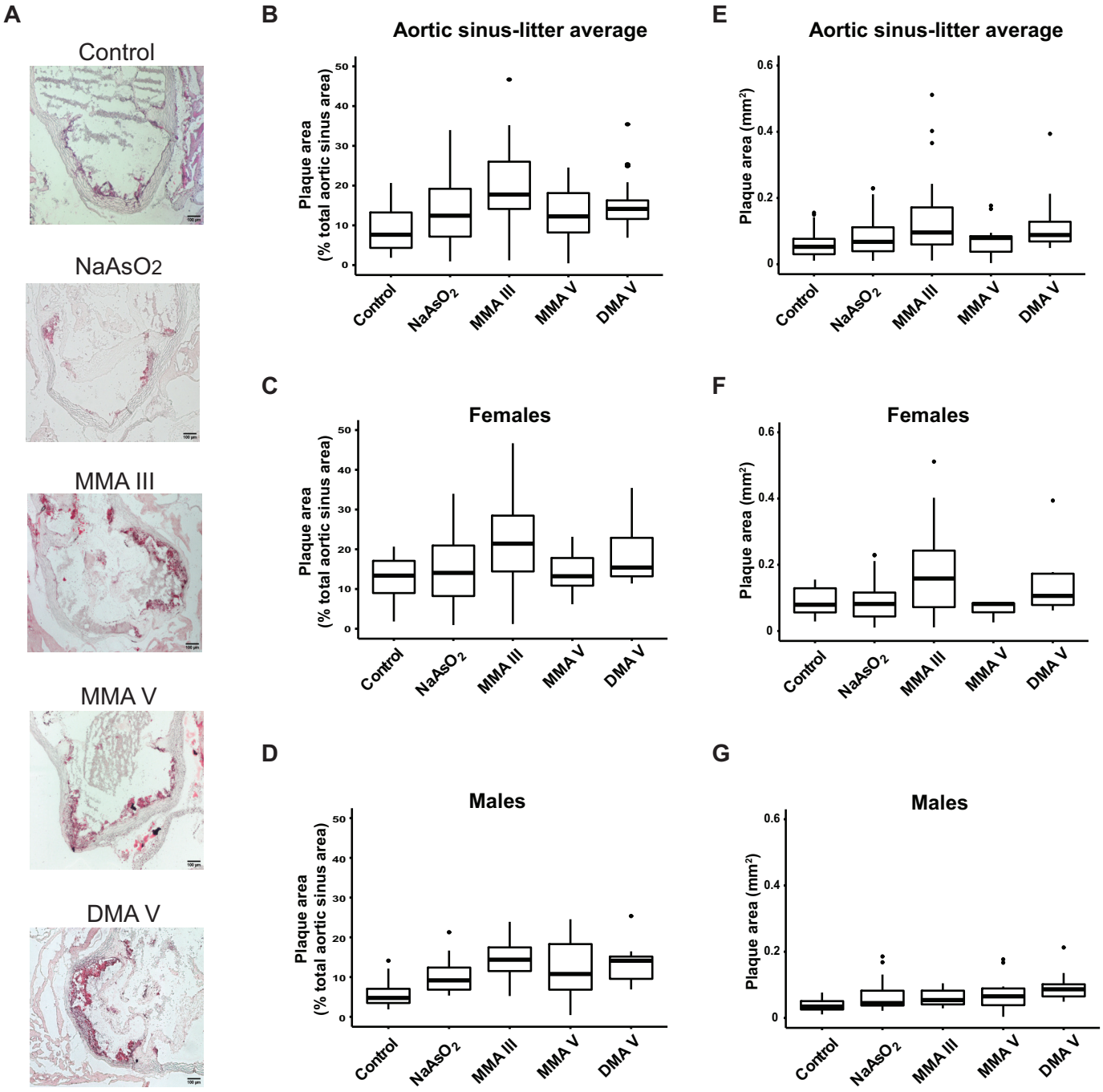

Figure 2. Differences in plaque formation in the aortic sinus in adult apoE$^{-/-}$ mice following early life arsenical exposure. ApoE$^{-/-}$ mice were exposed as described for Figure 1 and the plaque area in the aortic sinus was assessed by oil red O staining. The percentage of the lesion area of the aortic sinus was evaluated via oil red O staining. (A) Representative images. The box plots represent the distribution of unadjusted total lesion area as a percentage of total sinus area, where midline, box limits, whiskers, and dots denote the median, interquartile range, minimum and maximum values, and outliers, respectively. (B) The combined data set is presented, and sex-specific data sets for (C) females and (D) are presented. In addition, the lesion area was measured as millimeters squared, and the unadjusted data distribution for all the litters from (E) each exposed group as well as that separated by (F) female and (G) male offspring is shown. The corresponding numeric data are presented in Table S4 and that adjusted by litter are presented in Tables 2 and 3. Note: DMA^{V}, cacodylic acid; MMA^{III}, monomethylarsonous acid; MMA^{V}, disodium methyl arsonate hexahydrate; $NaAsO_2$, sodium arsenite.

Results

Analysis of Atherosclerotic Plaque Size following in Utero *Arsenic Exposure in an ApoE$^{-/-}$ Mouse Model*

We exposed mating pairs (i.e., both male and female parents) to 200-ppb arsenic as methylated arsenicals (MMA^{V}, MMA^{III}, or DMA^{V}), inorganic arsenic ($NaAsO_2$) or tap water. We continued exposure for 3 wk after birth so that subsequent litters of apoE$^{-/-}$ mice were exposed from mating to weaning, although arsenic may not be present in breast milk (Fängström et al. 2008; Islam et al. 2014). After weaning, all pups were kept on tap water until 18 wk of age, a time point at which postnatal exposure enhances lesion formation (Makhani et al. 2018). Table 1 shows the distribution of litter number, size, and sex. We did not find any differences in litter size between exposure groups but did find some differences in the proportion of males across exposure groups, confirming our decision to adjust for sex.

Table 2. Relative differences in the plaque size in aortic arch and sinus of arsenical-treated apoE$^{-/-}$ mice relative to their control counterparts and associated 95% confidence intervals (CIs), adjusted for sex.

	Lesion area					
	Percentage of total arch[a]		Percentage of aortic sinus[b]		Aortic sinus (mm^2)[c]	
Exposure groups	Relative difference (95% CI)	p-Value	Relative difference (95% CI)	p-Value	Relative difference (95% CI)	p-Value
$NaAsO_2$	2.6 (0.5, 4.6)	0.01	3.4 (0.1, 6.8)	0.04	0.02 (−0.02, 0.05)	0.40
MMA^{III}	10.4 (7.5, 13.2)	<0.001	9.6 (5.1, 14.1)	<0.001	0.07 (0.02, 0.12)	<0.01
MMA^{V}	7.7 (5.1, 10.3)	<0.001	3.7 (−0.6, 8.1)	0.09	0.01 (−0.04, 0.05)	0.69
DMA^{V}	8.4 (5.7, 11.0)	<0.001	6.9 (2.2, 11.5)	<0.01	0.06 (0.01, 0.10)	0.02

Note: Models were fitted using simple mixed regression models to control for the intra-litter correlation, and sex was included as a covariate. All exposure groups were compared with the unexposed (control) group for each outcome separately. The corresponding data distribution is depicted in Figures 1B and 2B,E. Number of apoE$^{-/-}$ litters (N) = Control: 12, $NaAsO_2$: 9, MMA^{III}: 4, MMA^{V}: 5; DMA^{V}: 5. DMA^{V}, cacodylic acid; MMA^{III}, monomethylarsonous acid; MMA^{V}, disodium methyl arsonate hexahydrate; $NaAsO_2$, sodium arsenite.
[a]Percentage of oil red O-stained area over the total arch area.
[b]Percentage of oil red O-stained lesion area over the total sinus area.
[c]Absolute lesion area as measured by oil red O staining.

We assessed atherosclerotic plaque size in the aortic arch (*en face)* and aortic sinus after staining with oil red O. Using a mixed-effects model, we found that the effects of arsenical treatment, with respect to the control group, varied by sex for many of the outcomes, that is, there was a statistically significant interaction ($p < 0.05$) between exposure groups and sex. Therefore, quantitative values for sex-wise analyses are reported in addition to litter averages for all the outcomes.

We observed that mean plaque size in the aortic arch and aortic sinus was larger in offspring of the dams exposed to either inorganic arsenic or its methylated intermediates. Figures 1 and 2 show box plots of the distributions of unadjusted results, and Table 2 shows the results adjusted for sex using the mixed models. Atherosclerotic lesions in the aortic arch were larger in the inorganic arsenic group by 2.6% [(95% CI: 0.5, 4.6%); $p = 0.01$] and that in sinus was larger by 3.4% [(95% CI: 0.1, 6.8%); $p = 0.04$] or by 0.02 mm^2 [(95% CI: −0.02, 0.05); $p = 0.40$] compared with the control group. Surprisingly, methylated arsenical exposures were significantly associated with the enhanced size of the aortic arch lesions [relative differences = 10.4% (95% CI: 7.5, 13.2%) for MMA^{III}, 7.7% (95% CI: 5.1, 10.3%) for MMA^{V}, and 8.4% (95% CI: 5.7, 11.0%) for DMA^{V})], as well as aortic sinus plaques [relative differences = 9.6% (95% CI: 5.1, 14.1%) for MMA^{III}, 3.7% (95% CI: −0.6, 8.1%) for MMA^{V}, and 6.9% (95% CI: 2.2, 11.5%) for DMA^{V}], which tended to be larger than $NaAsO_2$-induced plaques, particularly in the arch analyses (Figures 1 and 2 and Tables 2 and S4). For the aortic arch, we found an interaction ($p < 0.01$) between sex and the exposure groups. Therefore, we analyzed each sex separately, and we observed that the mean lesion size in the aortic arch was larger in both female and male offspring from arsenical-exposed dams; the effects of MMA^{III} were the largest in enhancing the plaques in females [relative difference = 13.6% (95% CI: 9.5, 17.6%)], whereas that of DMA^{V} were the largest in males [relative difference = 8.4% (6.0, 10.8%)] Figure 1 and Tables 3 and S4). In the aortic sinus, using percentages as outcome, we did not find any interaction between sex and the exposure groups ($p = 0.47$), and, therefore, the combined analysis is sufficient. We found rather different patterns of effects when we used the absolute area of the plaque in the aortic sinus measured in millimeters squared as the metric. There was an interaction by sex for the effects of arsenical treatments compared with the control group ($p = 0.02$). Here, the effects of MMA^{III} were the largest in enhancing plaques in the aortic sinus in females [relative difference = 0.10 mm^2 (95% CI: 0.03, 0.16 mm^2); $p < 0.01$], which is consistent with our observations for aortic arch analysis. Also consistent with arch data, we found a larger effect for DMA^{V} in enhancing the sinus plaque size in males [relative difference = 0.05 mm^2 (95% CI: 0.02, 0.09 mm^2); $p < 0.01$]. Moreover, we measured circulating concentrations of lipid and liver enzymes from the plasma of both male and female mice, and no differences were observed between control and arsenical-exposed mice (Tables S1 and S2).

Table 3. Differences in the plaque size in aortic arch and sinus of arsenical-treated apoE$^{-/-}$ mice relative to their control counterparts and associated 95% confidence intervals (CI), presented separately for females and males.

		Females		Males		
Outcomes	Exposure groups	Relative difference (95% CI)	p-Value	Relative difference (95% CI)	p-Value	$p_{Interaction}$ between males and females[a]
Lesion area (% of total arch)[b]	$NaAsO_2$	2.9 (−0.2, 6.0)	0.07	2.7 (0.7, 3.8)	0.01	<0.01
	MMA^{III}	13.6 (9.5, 17.6)	<0.001	7.6 (4.8, 10.5)	<0.001	
	MMA^{V}	8.2 (4.1, 12.3)	<0.001	7.3 (4.9, 9.6)	<0.001	
	DMA^{V}	8.6 (4.4, 12.9)	<0.001	8.4 (6.0, 10.8)	<0.001	
Lesion area (% of total sinus)[c]	$NaAsO_2$	2.7 (−3.6, 8.9)	0.38	4.9 (1.8, 7.9)	<0.001	0.47
	MMA^{III}	9.3 (1.4, 17.2)	0.02	8.8 (4.6, 13.1)	<0.001	
	MMA^{V}	1.1 (−7.4, 9.5)	0.80	5.9 (2.6, 9.3)	<0.001	
	DMA^{V}	7.4 (−1.9, 16.7)	0.11	7.7 (4.1, 11.2)	<0.001	
Lesion area (in aortic sinus) (mm^2)[d]	$NaAsO_2$	0.01 (−0.04, 0.06)	0.78	0.03 (0, 0.06)	0.06	0.02
	MMA^{III}	0.10 (0.03, 0.16)	<0.01	0.02 (−0.02, 0.06)	0.23	
	MMA^{V}	−0.02 (−0.09, 0.05)	0.56	0.03 (0, 0.06)	0.07	
	DMA^{V}	0.07 (−0.01, 0.15)	0.08	0.05 (0.02, 0.09)	<0.01	

Note: To obtain sex-specific changes, separate models were fitted for females and males using simple mixed regression to control for the intra-litter correlation. All exposure groups were compared with the unexposed (control) group, for each outcome. DMA^{V}, cacodylic acid; MMA^{III}, monomethylarsonous acid; MMA^{V}, disodium methyl arsonate hexahydrate; $NaAsO_2$, sodium arsenite.
[a]Interactions between sex and exposure groups were tested using maximum likelihood and the resulting p-values are presented here. The corresponding data distribution is depicted in Figures 1C,F and 2C,D and 2F,G.
[b]Percentage of oil red O-stained area over the total arch area; Number of apoE$^{-/-}$ litters (N) = Control: 12, $NaAsO_2$: 9, MMA^{III}: 4, MMA^{V}: 5; DMA^{V}: 5.
[c]Percentage of oil red O-stained lesion area over the total sinus area; Number of apoE$^{-/-}$ litters (N) = Control: 12, $NaAsO_2$: 9, MMA^{III}: 4, MMA^{V}: 4; DMA^{V}: 4.
[d]Absolute lesion area as measured by oil red O-staining; Number of apoE$^{-/-}$ litters (N) = Control: 12, $NaAsO_2$: 9, MMA^{III}: 4, MMA^{V}: 4; DMA^{V}: 4.

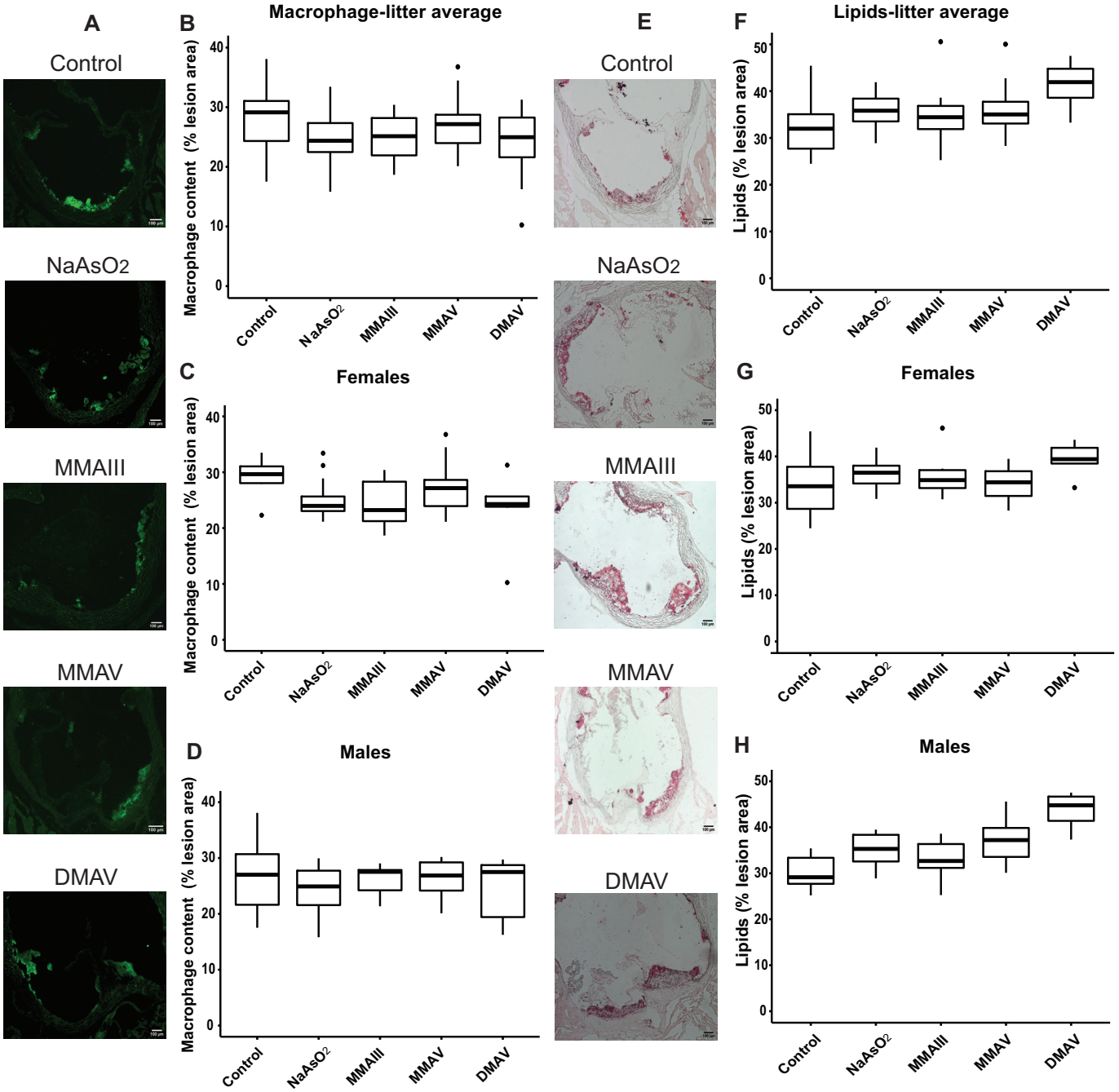

Figure 3. Differences in plaque macrophage and lipid content in the aortic sinus in adult apoE$^{-/-}$ mice following early life arsenical exposure. ApoE$^{-/-}$ mice were exposed as described for Figure 1. (A–D) Macrophage and (E–H) lipid content were evaluated in the aortic sinus relative to the total lesion area using Moma-2 and oil red O staining, respectively. (A) and (E) show representative images. Scale bar: 100 μm. (B) Box plots represent the data distribution of the unadjusted percentage of macrophages with respect to the total sinus area for all offspring in the control and arsenical-exposed groups, whereas those in (C) and (D) represent that in the female and male offspring, respectively. (E) Box plots represent the data distribution of the unadjusted percentage of lipid content with respect to the total sinus area for all offspring in the control and arsenical-exposed groups, whereas (F) and (G) represent that in the female and male offspring, respectively. The midline, box limits, whiskers, and dots denote the median, interquartile range, minimum and maximum values, and outliers, respectively. The corresponding numeric data are presented in Table S5 and that adjusted by litter are presented in Tables 4 and 5. Note: DMA^{V}, cacodylic acid; MMA^{III}, monomethylarsonous acid; MMA^{V}, disodium methyl arsonate hexahydrate; $NaAsO_2$, sodium arsenite.

Analysis of Atherosclerotic Plaque Components following in Utero *Arsenical Exposure in an ApoE$^{-/-}$ Mouse Model*

We assessed both macrophage and lipid content in the plaques following *in utero* and early life arsenic exposure. No statistically significant associations between macrophage content and arsenical exposure were observed, although all exposure groups showed a lower percentage of macrophages compared with the untreated control (Figure 3A–D and Tables 4 and S5). Importantly, the *in utero* exposure to inorganic and methylated arsenicals led to higher mean lipid content within the plaque (Figure 3E–H and Tables 4 and S5), with the DMA^{V}-exposed group being statistically significant [relative difference = 9.9% (95% CI: 4.9, 14.8%); $p < 0.001$]. For plaque lipid content, we found an interaction ($p = 0.02$) between sex and exposure groups. Therefore, analyzing each sex separately, we found a larger effect

Table 4. Differences in the plaque components (macrophages, lipids, smooth muscle cells, and collagen) in aortic sinus of arsenical-treated apoE$^{-/-}$ mice relative to their control counterparts and associated 95% confidence intervals (CIs), adjusted for sex.

	Macrophages (% of sinus lesion area)[a]		Lipids (% of sinus lesion area)[b]		SMCs (% of sinus lesion area)[c]		Collagen (% of sinus lesion area)[d]	
Groups	Relative differences (95% CI)	p-Value	Relative differences (95% CI)	p-Value	Relative differences (95% CI)	p-Value	Relative differences (95% CI)	p-Value
$NaAsO_2$	−3.0 (−7.2, 1.2)	0.16	3.8 (−0.8, 8.4)	0.10	−2.2 (−6.9, 2.5)	0.35	−0.6 (−9.4, 8.2)	0.89
MMA^{III}	−2.8 (−7.4, 1.8)	0.22	2.7 (−2.1, 7.6)	0.24	−2.6 (−7.9, 2.7)	0.32	0.4 (−8.6, 9.3)	0.93
MMA^{V}	−1.1 (−5.9, 3.7)	0.63	3.5 (−1.08, 8.1)	0.12	−2.1 (−7.6, 3.4)	0.43	−1.3 (−9.5, 6.9)	0.74
DMA^{V}	−3.3 (−8.0, 1.3)	0.15	9.9 (4.9, 14.8)	<0.001	−4.3 (−10.0, 1.5)	0.13	−6.2 (−15.4, 2.8)	0.16

Note: Models were fitted using simple mixed regression models to control for the intra-litter correlation, and sex was included as a covariate. All exposure groups were compared with the unexposed (control) group, for each outcome separately. The corresponding data distribution is depicted in Figures 3B,F and 4B,F. DMA^{V}, cacodylic acid; MMA^{III}, monomethylarsonous acid; MMA^{V}, disodium methyl arsonate hexahydrate; $NaAsO_2$, sodium arsenite; SMAα, smooth muscle actin-alpha.

[a]Percentage of Moma-2 antibody-stained area over the total lesion area in the aortic sinus as measured by the intensity of fluorescent signal at 488 nm; Number of apoE$^{-/-}$ litters (N) = Control: 6, $NaAsO_2$: 3, MMA^{III}: 4, MMA^{V}: 3; DMA^{V}: 4.

[b]Percentage of oil red O-stained area over the total lesion area in the aortic sinus; Number of apoE$^{-/-}$ litters (N) = Control: 6, $NaAsO_2$: 3, MMA^{III}: 4, MMA^{V}: 3; DMA^{V}: 4.

[c]Percentage of total SMAα antibody-stained area over the total lesion area in the aortic sinus as measured by the intensity of fluorescent signal at 488 nm; Number of apoE$^{-/-}$ litters (N) = Control: 6, $NaAsO_2$: 3, MMA^{III}: 4, MMA^{V}: 3; DMA^{V}: 3.

[d]Percentage of picrosirius red-stained area over the total lesion area in the aortic sinus; Number of apoE$^{-/-}$ litters (N) = Control: 6, $NaAsO_2$: 3, MMA^{III}: 3, MMA^{V}: 3; DMA^{V}: 3.

for MMA^{V} and DMA^{V} in males as compared with the respective unexposed controls [relative differences = 6.6% (95% CI: 1.2, 12.0%); $p = 0.02$ for MMA^{V} and 13.4% (95% CI: 7.6, 19.1%); $p < 0.01$ for DMA^{V}] (Figure 3G vs. 3H and Tables 5 and S5).

We also investigated collagen and SMC content using histological techniques. The mean percentage of SMCs and collagen measurement had a wide variability and did not differ between the arsenical-exposed groups and the control group (Figure 4A–D,E–H, and Tables 4 and S5). Despite not finding an overall effect, we observed an interaction between sex and exposure groups for both of these outcomes (Tables 5 and S5). When males and females were considered separately for plaque collagen content, DMA^{V} had the largest effect on male offspring in that it resulted in profoundly lesser collagen in the exposed males [relative difference = − 16.1% (95% CI: −25.4, −6.7%); $p < 0.01$], whereas in females, $NaAsO_2$ had the largest effect but resulted in more plaque collagen content instead [relative difference = 8.0 (95% CI: 1.0, 15.0%); $p < 0.05$] (Tables 5 and S5).

Analysis of Atherosclerotic Plaque Formation following in Utero *Arsenic Exposure in an ApoE$^{-/-}$/As3MT$^{-/-}$ Mouse Model*

We investigated the impact of the biotransformation process on atherosclerotic plaques after *in utero* and early life exposure. We used our DKO mice, which have proven useful to study the effects of arsenic methylation in arsenic-induced atherosclerosis (Negro Silva et al. 2017). DKO mice were exposed from mating to weaning to 200-ppb $NaAsO_2$ or tap water. Atherosclerotic plaques were assessed after 13 wk on tap water. Interestingly, $NaAsO_2$ did not have an effect on lesion area in the aortic arch [relative difference = 1.3% (95% CI: −5.2, 7.9%)] (Figure 5 and Tables 6 and S6) or on plaque size in the aortic sinus [relative differences = − 1.66% (95% CI: −7.0, 3.6%) or −0.0003 mm^2 (95% CI: −0.07, 0.07 mm^2)] in DKO mice (Figures 6 and Tables 6 and S6). As well, we did not find an

Table 5. Differences in the plaque components (macrophages, lipids, smooth muscle cells, and collagen) in the aortic sinus of arsenical-treated apoE$^{-/-}$ mice relative to their control counterparts and associated 95% confidence intervals (CIs), presented separately for females and males.

		Females		Males		
Outcome	Exposure groups	Relative difference (95% CI)	p-Value	Relative difference (95% CI)	p-Value	$p_{Interaction}$ between males and females[a]
Macrophage (% of sinus lesion area)[b]	$NaAsO_2$	−3.8 (−9.7, 2.2)	0.19	−2.6 (−9.2, 3.9)	0.40	0.42
	MMA^{III}	−4.5 (−10.4, 1.4)	0.12	−0.8 (−7.5, 6.0)	0.80	
	MMA^{V}	−1.5 (−7.7, 4.7)	0.61	−0.6 (−7.2, 6.0)	0.85	
	DMA^{V}	−6.7 (−13.3, 0)	0.05	−2.0 (−8.2, 4.2)	0.50	
Lipids (% of sinus lesion area)[c]	$NaAsO_2$	2.2 (−6.6, 11.0)	0.59	5.0 (−0.5, 10.5)	0.07	0.02
	MMA^{III}	2.0 (−7.0, 11.0)	0.63	3.2 (−2.5, 8.8)	0.25	
	MMA^{V}	0.7 (−8.1, 9.5)	0.86	6.6 (1.2, 12.0)	0.02	
	DMA^{V}	6.1 (−3.8, 16.1)	0.20	13.4 (7.6, 19.1)	<0.01	
Smooth muscle cells (% of sinus lesion area)[d]	$NaAsO_2$	0.4 (−4.2, 5.0)	0.84	−8.0 (−17.3, 1.3)	0.09	<0.01
	MMA^{III}	−1.2 (−5.9, 3.6)	0.61	−2.7 (−12.0, 6.7)	0.55	
	MMA^{V}	0.2 (−4.5, 5.04)	0.91	−3.7 (−13.0, 5.6)	0.41	
	DMA^{V}	−2.0 (−7.5, 3.5)	0.45	−7.0 (−16.5, 2.4)	0.13	
Collagen (% of sinus lesion area)[e]	$NaAsO_2$	8.0 (1.0, 15.0)	0.03	−8.8 (−17.8, 0.2)	0.05	<0.01
	MMA^{III}	6.5 (−1.1, 14.0)	0.08	−4.7 (−13.9, 4.6)	0.29	
	MMA^{V}	2.9 (−4.1, 10.0)	0.37	−5.6 (−14.0, 2.8)	0.18	
	DMA^{V}	5.9 (−2.2, 14.0)	0.14	−16.1 (−25.4, −6.7)	<0.01	

Note: To obtain sex-specific changes, separate models were fitted for females and males using simple mixed regression to control for the intra-litter correlation. All exposure groups were compared with the unexposed (control) group, for each outcome. DMA^{V}, cacodylic acid; MMA^{III}, monomethylarsonous acid; MMA^{V}, disodium methyl arsonate hexahydrate; $NaAsO_2$, sodium arsenite; SMAα, smooth muscle actin-alpha.

[a]Interactions between sex and exposure groups were tested using maximum likelihood and the resulting p-values are presented here. The corresponding data distribution is depicted in Figures 3C,D, 3G,H, 4C,D, and 4G,H.

[b]Percentage of Moma-2 antibody-stained area over the total lesion area in the aortic sinus as measured by the intensity of fluorescent signal at 488 nm; Number of apoE$^{-/-}$ litters (N) = Control: 6, $NaAsO_2$: 3, MMA^{III}: 4, MMA^{V}: 3; DMA^{V}: 4.

[c]Percentage of oil red O-stained area over the total lesion area in the aortic sinus; Number of apoE$^{-/-}$ litters (N) = Control: 6, $NaAsO_2$: 3, MMA^{III}: 4, MMA^{V}: 3; DMA^{V}: 4.

[d]Percentage of total SMAα antibody-stained area over the total lesion area in the aortic sinus as measured by the intensity of fluorescent signal at 488 nm; Number of apoE$^{-/-}$ litters (N) = Control: 6, $NaAsO_2$: 3, MMA^{III}: 4, MMA^{V}: 3; DMA^{V}: 3.

[e]Percentage of picrosirius red-stained area over the total lesion area in the aortic sinus; Number of apoE$^{-/-}$ litters (N) = Control: 6, $NaAsO_2$: 3, MMA^{III}: 3, MMA^{V}: 3; DMA^{V}: 3.

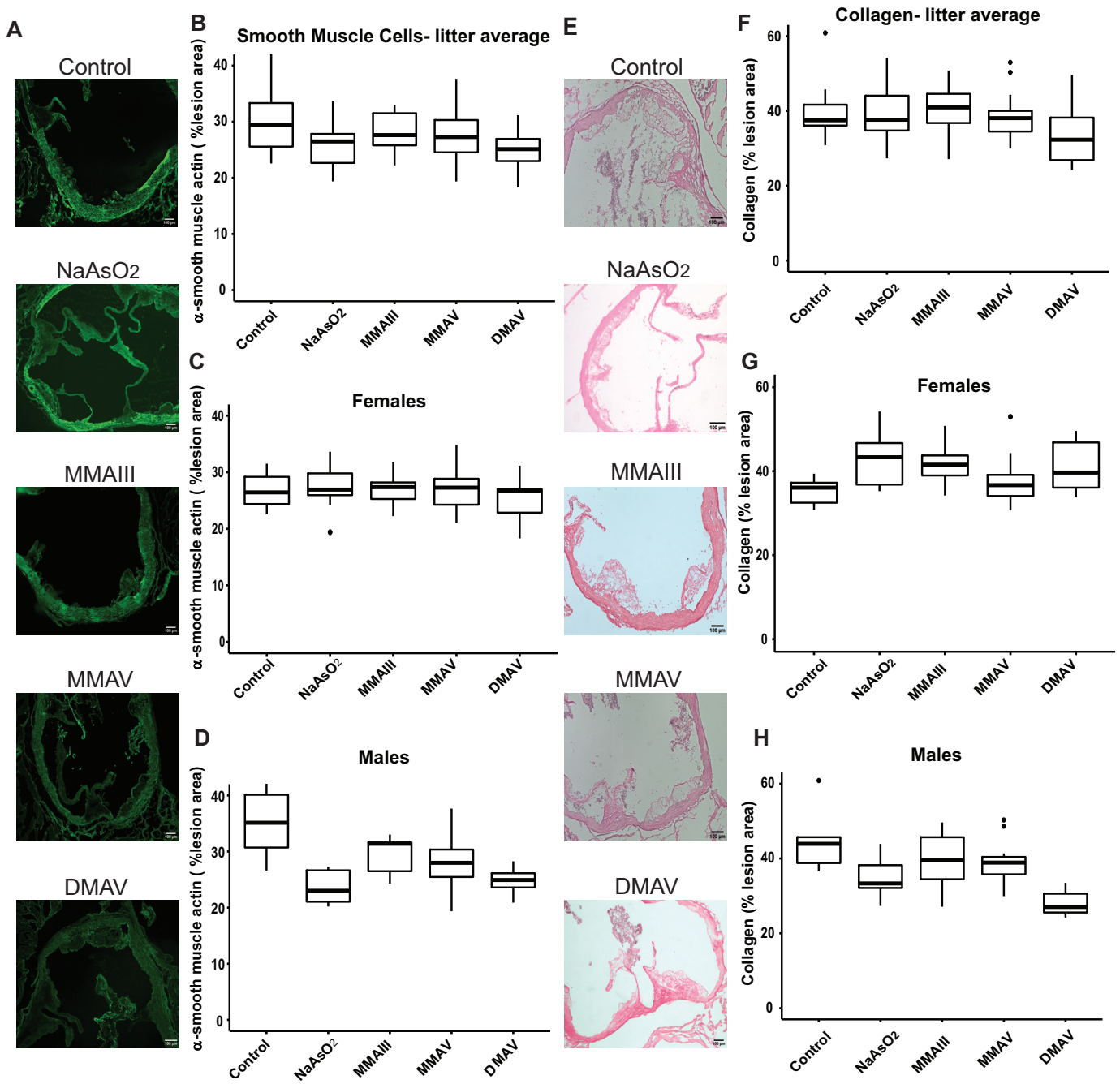

Figure 4. Differences in plaque SMC and collagen content in the aortic sinus in adult apoE$^{-/-}$ mice following early life arsenical exposure. ApoE$^{-/-}$ mice were exposed as described for Figure 1. (A–D) SMC and (E–H) collagen content were evaluated in the aortic sinus relative to the total lesion area using α-smooth muscle actin and picrosirius red staining, respectively. Scale bar: 100 μm. (B) Represents the data distribution of the unadjusted percentage of SMCs with respect to the total sinus area for all offspring in the control and arsenical-exposed groups, whereas (C) and (D) represent that in the female and male offspring, respectively. (E) Represents the data distribution of the unadjusted percentage of collagen content with respect to the total sinus area for all offspring in the control and arsenical-exposed groups, whereas (F) and (G) represent that in the female and male offspring, respectively. The midline, box limits, whiskers, and dots denote the median, interquartile range, minimum and maximum values, and outliers, respectively. The corresponding numeric data are presented in Table S5 and that adjusted by litter are presented in Tables 4 and 5. Note: DMA^{V}, cacodylic acid; MMA^{III}, monomethylarsonous acid; MMA^{V}, disodium methyl arsonate hexahydrate; $NaAsO_2$, sodium arsenite; SMC, smooth muscle cell.

interaction between sex and the arsenic exposure for either of these outcomes (Table 7). Similar to apoE$^{-/-}$ mice, female DKO mice had larger plaques than male DKO mice, independent of the exposure, although there was a large variability in plaque size in the DKO cohorts (Figures 5 and 6). Of note, the basal levels of plaque in the control DKO mice were significantly higher than that of control apoE$^{-/-}$ mice (Figures 5 and 6 and Table S3).

Discussion

Arsenic is an environmental toxicant to which millions of people are exposed worldwide (Naujokas et al. 2013). Previously, we and others have shown that postnatal exposure to both inorganic (Lemaire et al. 2014, 2011; Simeonova et al. 2003; Srivastava et al. 2009) and methylated arsenicals (Negro Silva

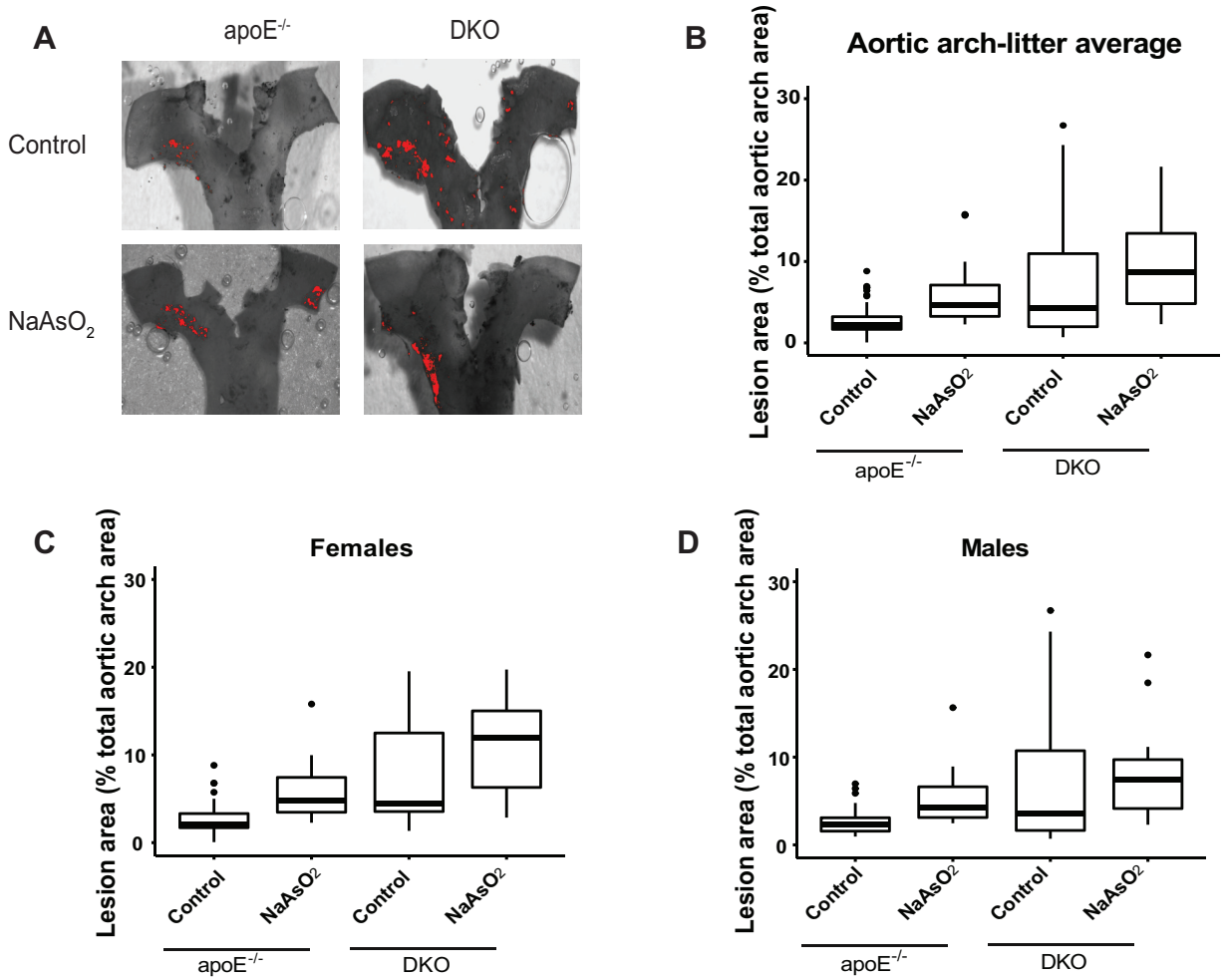

Figure 5. Differences in plaque formation in the aortic arch in adult apoE$^{-/-}$/As3MT$^{-/-}$ DKO mice following early life arsenical exposure. ApoE$^{-/-}$ or DKO mice were exposed to 200 ppb $NaAsO_2$ or maintained on tap water from conception to weaning. After weaning (4 wk), animals were kept on tap water for an additional 13 wk. The percentage of the lesion area of the aortic arch was evaluated via oil red O staining. (A) Representative images. Scale bar: 100 μm. The box plots represent the distribution of unadjusted total lesion area as a percentage of total arch area. (B) The combined data set is presented, and sex-specific data sets for (C) females and (D) are presented. The midline, box limits, whiskers, and dots denote the median, interquartile range, minimum and maximum values, and outliers, respectively. The corresponding numeric data are presented in Table S6 and that adjusted by litter are presented in Tables 6 and 7. Note: DKO, double-knock out; $NaAsO_2$, sodium arsenite.

et al. 2017) was pro-atherogenic in apoE$^{-/-}$ mice. Here, we provide evidence that combined pre- and perinatal exposure to moderate concentrations of these compounds also promotes atherosclerosis. These data complement other studies that have shown that early life exposure to arsenic correlated with disease later in life (Bailey and Fry 2014; Chen et al. 2019; Steinmaus et al. 2016). Importantly, these methylated arsenicals appear to be as pro-atherogenic as the parent compounds, indicating that the differences in methylation efficiency conferred by As3MT polymorphisms may not be relevant in this exposure scenario.

One criticism of previous murine transplacental models to show intergenerational effects was that high concentrations (42,500–200,000 ppb arsenic) were employed (Garry et al. 2015). The groundbreaking studies observing cancer outcomes following *in utero* exposure to arsenic in mice used 42,500 and 85,000 ppb arsenic (Waalkes et al. 2003). Arsenic exposure (45,000 ppb) during pregnancy increased the early onset of

Table 6. Differences in the plaque size in the aortic arch and the sinus in the apoE$^{-/-}$/As3MT$^{-/-}$ DKO mouse model in response to arsenic exposure in *utero* relative to their control counterpart and associated 95% confidence intervals (CIs), adjusted for sex.

	Lesion area					
	Percentage of aortic arch[a]		Percentage of aortic sinus[b]		Aortic sinus (mm^2)[c]	
Exposure group	Relative difference (95% CI)	*p*-Value	Relative difference (95% CI)	*p*-Value	Relative difference (95% CI)	*p*-Value
$NaAsO_2$	1.3 (−5.2, 7.9)	0.67	−1.66 (−7.0, 3.6)	0.50	−0.0003 (−0.07, 0.07)	0.99

Note: Models were fitted using simple mixed regression models to control for the intra-litter correlation, and sex was included as a covariate. All exposure groups were compared with the unexposed (control) group, for each outcome separately. The corresponding data distribution is depicted in Figures 5B, 6B and 6E. DKO, double-knock out; $NaAsO_2$, sodium arsenite; Number of DKO litters (N) = Control: 4, $NaAsO_2$: 4.
[a]Percentage of oil red O-stained area over the total arch area.
[b]Percentage of oil red O-stained lesion area over the total sinus area.
[c]Absolute lesion area as measured by oil red O staining.

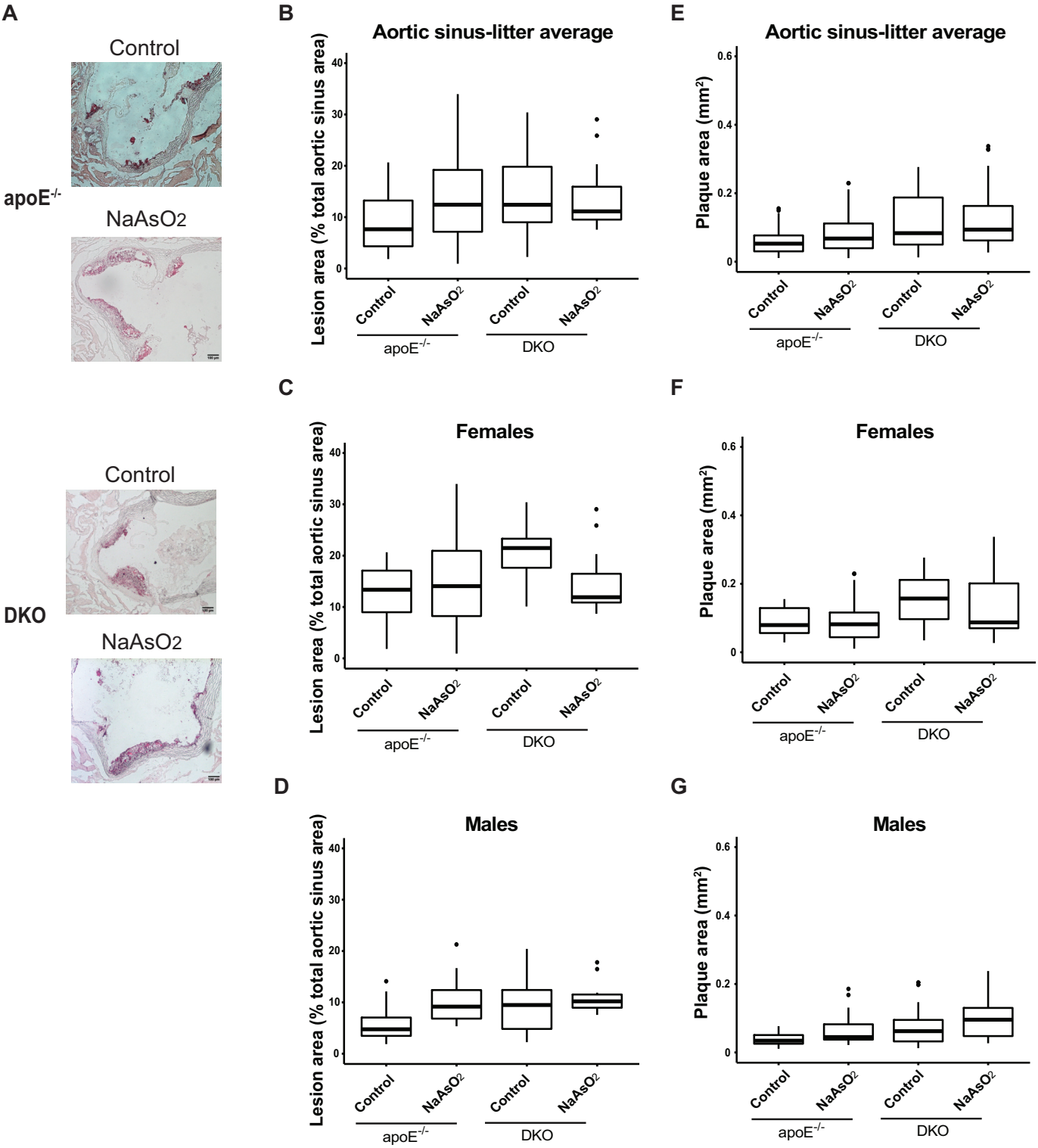

Figure 6. Differences in plaque formation in the aortic sinus in adult apoE$^{-/-}$ As3mt$^{-/-}$ DKO mice following early life arsenical exposure. ApoE$^{-/-}$ or DKO mice were exposed as described for Figure 1 and the plaque area in the aortic sinus was assessed by oil red O staining. The percentage of the lesion area of the aortic sinus was evaluated via oil red O staining. (A) Representative images. The box plots represent the distribution of unadjusted total lesion area as a percentage of the total sinus area, where midline, box limits, whiskers, and dots denote the median, interquartile range, minimum and maximum values, and outliers respectively, in the data set. (B) The combined data set is presented, and sex-specific data sets for (C) females and (D) are presented. In addition, the lesion area was also measured as millimeters squared, and the unadjusted data distribution for all the litters from (E) each exposed group as well as that separated by (F) female and (G) male offspring is shown. The corresponding numeric data are presented in Table S6 and that adjusted by litter are presented in Tables 6 and 7. Note: DKO, double-knock out; DMA^{V}, cacodylic acid; MMA^{III}, monomethylarsonous acid; MMA^{V}, disodium methyl arsonate hexahydrate; $NaAsO_2$, sodium arsenite.

Table 7. Differences in the plaque size in the aortic arch and the sinus in the apoE$^{-/-}$/As3MT$^{-/-}$ DKO mouse model in response to $NaAsO_2$ exposure *in utero* relative to their control counterpart and associated 95% confidence intervals (CIs), presented separately for females and males.

Outcome	Females		Males		$p_{Interaction}$ between males and females[a]
	Relative differences (95% CI)	*p*-Value	Relative differences (95% CI)	*p*-Value	
Lesion area (% of total arch area)[b]	1.2 (−6.6, 9.1)	0.73	1.8 (−6.5, 10.2)	0.64	0.70
Lesion area (% of total arch area)[c]	−4.2 (−11.9, 3.4)	0.24	1.2 (−4.4, 6.8)	0.64	0.11
Lesion area (in aortic sinus) (mm^2)[d]	0.009 (−0.12, 0.14)	0.87	0.024 (−0.04, 0.08)	0.39	0.73

Note: To obtain sex-specific changes, separate models were fitted for females and males using simple mixed regression to control for the intra-litter correlation. All exposure groups were compared with the unexposed (control) group, for each outcome. Number of litters DKO (N) = Control: 4, $NaAsO_2$: 4. DKO, double-knock out; $NaAsO_2$, sodium arsenite.
[a]Interactions between sex and exposure groups were tested using maximum likelihood and the resulting *p*-values are presented here. The corresponding data distribution is depicted in Figures 5C,D, 6C,D, and 6F,G.
[b]Percentage of oil red O-stained area over the total arch area.
[c]Percentage of oil red O-stained lesion area over the total sinus area.
[d]Absolute lesion area as measured by oil red O staining.

atherosclerosis in the apoE$^{-/-}$ mouse model (Srivastava et al. 2007; States et al. 2012). Our present study extends these findings to 200 ppb arsenic as inorganic, $NaAsO_2$, and as methylated arsenicals. Thus, at least for atherosclerosis, moderate concentrations resulted in larger plaques and a similar disease phenotype as high concentrations in mice. An important consideration is that mice metabolize arsenic more quickly than humans (ATSDR 2007), thus making an extrapolation to exposed human populations difficult. Arguably, a 200-ppb arsenic exposure in mice approximates a 40-ppb exposure in humans using the human equivalent dose calculations described by the U.S. Food and Drug Administration (FDA 2005). Thus, the data presented here are relevant to low-level, more prevalent exposure groups and suggest that populations living in arsenic-endemic areas may have adverse generational health effects despite remediation of arsenic contamination from their waters.

Here, we show that a conception-to-early life exposure to arsenicals can significantly enhance atherosclerotic plaque sizes in the aortic arch and sinus in the apoE$^{-/-}$ mouse model. These effects are similar to what we observed in our postnatal exposure model (Negro Silva et al. 2017). Of note, an early life exposure to methylated arsenicals resulted in larger plaque sizes as compared with $NaAsO_2$-exposed mice, whereas in postnatal exposures, $NaAsO_2$ had pro-atherogenic effects equal to or greater than methylated arsenicals (Negro Silva et al. 2017). We had observed *in vitro* (Padovani et al. 2010) and after a 13-wk-long postnatal exposure *in vivo* (Lemaire et al. 2011; Negro Silva et al. 2017) that arsenic impaired lipid handling in macrophages. Individual macrophages retained more lipids because of diminished cholesterol efflux (Lemaire et al. 2014). In the present study, we observed elevated plaque lipids without a concomitant difference in plaque macrophage contents, which is also consistent with our previous findings. SMCs and collagen are also components of the plaque and promote plaque stability (Libby et al. 2011). We previously reported that postnatal arsenical exposure decreased SMCs and collagen (Lemaire et al. 2011; Negro Silva et al. 2017), characteristic of plaques more prone to rupture (Gomez and Owens 2012; Libby et al. 2011). In the present study, we observed lower numbers of SMCs and less collagen content in treated vs. control mice in males, but not females. It is difficult to say how this would translate to humans given that the sex differences observed in apoE$^{-/-}$ mice are opposite of what is observed in humans (i.e., in mice, females have larger plaques, whereas in humans, males do). There is some literature indicating that sex is a determinant in the response to arsenic in terms of metabolic diseases. For instance, a population-based study of the residents in Central Italy exposed to low-to-medium doses of arsenic concluded that males had a higher mortality hazard ratio of arsenic-associated myocardial infarctions than females, whereas the inverse was true for diabetes (D'Ippoliti et al. 2015). This sexual dimorphism can be attributed to direct as well as indirect factors. For instance, arsenic induced sex-specific changes of the gut microbiome in mice (Chi et al. 2016) and humans (Hoen et al. 2018), which had been correlated with metabolic health (Peng et al. 2020). Moreover, epidemiologic data has suggested that women have higher arsenic methylation rates than men as measured by their urinary arsenical profile, although this effect is lost in older women (Lindberg et al. 2008). This not only suggests a role of arsenic methylation efficiency in sexually dimorphic effects of arsenic, but also implicates sex hormones as a potential factor. However, these findings are based on arsenic species measured in urine samples only. More specifically, both the gut microbiome (Chi et al. 2019) and As3MT activity (Negro Silva et al. 2017) have been linked to arsenic-induced dyslipidemia and atherosclerosis in mouse models, providing potential explanations for our observations. Furthermore, sex-specific differences were observed following *in utero* arsenic exposure in humans. For instance, the placentae in female fetuses had a higher expression of the arsenic transporter AQP9 (Winterbottom et al. 2017). *In utero* arsenic exposure led to decreased birth weight, but only in males (Xu et al. 2011). Besides, arsenic-associated changes in cognitive functions differed between sexes (Hamadani et al. 2011). Together, these data support our findings that *in utero* and early life arsenic exposure is linked to sex-specific differences in CVD later in life.

Our data show that mice lacking As3MT have a higher basal level of atherosclerotic plaque in the absence of drinking-water–derived arsenic exposure. This may be explained by a higher arsenic accumulation from laboratory diet in the absence of As3MT-dependent metabolism compared with As3MT wild-type mice although we did use a purified diet to minimize the amount of arsenic contributed through the food. Therefore, the impact of arsenic biotransformation on atherosclerosis is difficult to decipher in this study, as we observed slightly larger, but statistically insignificant, plaques in the aortic arch and no change in plaque size in the aortic sinus (Figures 5 and 6). Arsenic biotransformation has recently received attention in regard to its potential in arsenic pathogenesis (Chen et al. 2013a; Kuo et al. 2017). We were the first group to show that As3MT is required for arsenic-enhanced atherosclerosis following a postnatal exposure in mice (Negro Silva et al. 2017). Herein, we used our DKO model to investigate the effects of As3MT deletion on the outcomes that we had observed after prenatal exposure to inorganic arsenic in apoE$^{-/-}$ mice (Figure 1). One hypothesis is that dimethylarsenous acid (DMA^{III}) or other methylated intermediates may drive the effects. MMA^{III}, MMA^{V}, and DMA^{V} were unable to induce atherosclerosis in our postnatal exposure model in DKO mice (Negro Silva et al. 2017), but it is possible that *in utero* exposure could be pro-atherogenic. However, these exposures were not tested in the present study. Several epidemiologic studies have correlated arsenic metabolism patterns with adverse health outcomes in at-risk populations. Recent reports from the Strong

Heart Family Study showed a correlation between arsenic metabolite ratios (high DMA% and low MMA%) and the incidence of metabolic syndrome, as well as with greater waist circumference, a risk factor for CVDs, independent of arsenic exposure (Spratlen et al. 2018). Incomplete arsenic methylation (higher urinary MMA/DMA ratios) in humans was also associated with atherosclerosis in adults (Chen et al. 2013a) and with the risk of CVD (Chen et al. 2013b; Kuo et al. 2017). Interestingly, genetic variants in the 10q24.32 region near As3MT were important determinants of arsenic metabolism patterns and disease outcomes (Balakrishnan et al. 2017). For instance, distinct genetic variants in this locus were associated with arsenic metabolism efficiency as determined by urinary arsenic metabolites (Chernoff et al. 2020), as well as with the risk of skin lesions among unrelated individuals in Bangladesh (Pierce et al. 2012). Hence, the urinary arsenic profile, a surrogate for arsenic metabolism efficiency, can be an important biomarker to predict disease susceptibility associated with the As3MT locus and can have translational implications in the prevention of arsenic-associated toxicities.

In summary, our results show that methylated arsenicals were pro-atherogenic following early life exposure and that the biotransformation process was an important mechanism driving this phenotype. In addition, our data suggest that epidemiologic studies should evaluate single nucleotide polymorphisms that affect arsenic methylation efficiency in relation to *in utero* exposure when evaluating arsenic-exposed populations. Finally, our data further support the need to understand the mechanism by which arsenic enhances atherosclerosis in order to define appropriate interventions because, clearly, removal of arsenic is not enough to reverse damage caused by *in utero* exposure.

Acknowledgments

This work was supported by a grant from the Canadian Institutes of Health Research (MOP-115000; K.K.M.) and the Heart and Stroke Foundation (G-17-00018365; K.K.M.). L.F.N.S. and K.K.M. were supported by Gordon Phillips Fellowship/McGill Faculty of Medicine and TD bank/LDI fellowship.

References

ATSDR (Agency for Toxic Substances and Disease Registry). 2007. *Toxicological Profile for Arsenic*. Atlanta, GA: U.S. Department of Health and Human Services, Public Health Service. 2007. https://stacks.cdc.gov/view/cdc/11481 [accessed 16 April 2021].

Bailey K, Fry RC. 2014. Long-term health consequences of prenatal arsenic exposure: links to the genome and the epigenome. Rev Environ Health 29(1–2):9–12, PMID: 24552957, https://doi.org/10.1515/reveh-2014-0006.

Balakrishnan P, Vaidya D, Franceschini N, Voruganti VS, Gribble MO, Haack K, et al. 2017. Association of cardiometabolic genes with arsenic metabolism biomarkers in American Indian communities: the Strong Heart Family Study (SHFS). Environ Health Perspect 125(1):15–22, PMID: 27352405, https://doi.org/10.1289/EHP251.

Bates D, Maechler M, Bolker B, Walker S. 2014a. lme4: linear mixed-effects models using Eigen and S4. Version 1.1-7.

Bieler G, Williams R. 1995. Cluster sampling techniques in quantal response teratology and developmental toxicity studies. Biometrics 51(2):764–776, PMID: 7662858, https://doi.org/10.2307/2532963.

Breslow NE, Clayton DG. 1993. Approximate inference in generalized linear mixed models. Journal of American Statistical Association 88(421):9–25, https://doi.org/10.1080/01621459.1993.10594284.

BGS (British Geological Survey). 2000. Executive summary of the main report of phase I, groundwater studies of As contamination in Bangladesh by British Geological Survey and Mott MacDonald (UK) for the Government of Bangladesh, Ministry of Local Government, Rural Development and Cooperatives DPHE and DFID (UK). http://bicn.com/acic/resources/infobank/bgs-mmi/risumm.htm [accessed 17 March 2021].

Caligiuri G, Nicoletti A, Zhou X, Tornberg I, Hansson GK. 1999. Effects of sex and age on atherosclerosis and autoimmunity in apoE-deficient mice. Atherosclerosis 145(2):301–308, PMID: 10488957, https://doi.org/10.1016/S0021-9150(99)00081-7.

Chen Y, Wu F, Liu X, Parvez F, Lolacono NJ, Gibson EA, et al. 2019. Early life and adolescent arsenic exposure from drinking water and blood pressure in adolescence. Environ Res 178:108681, PMID: 31520830, https://doi.org/10.1016/j.envres.2019.108681.

Chen Y, Wu F, Liu M, Parvez F, Slavkovich V, Eunus M, et al. 2013a. A prospective study of arsenic exposure, arsenic methylation capacity, and risk of cardiovascular disease in Bangladesh. Environ Health Perspect 121(7):832–838, PMID: 23665672, https://doi.org/10.1289/ehp.1205797.

Chen Y, Wu F, Parvez F, Ahmed A, Eunus M, McClintock TR, et al. 2013b. Arsenic exposure from drinking water and QT-interval prolongation: results from the health effects of arsenic longitudinal study. Environ Health Perspect 121(4):427–432, PMID: 23384555, https://doi.org/10.1289/ehp.1205197.

Chernoff M, Tong L, Demanelis K, Vander Griend D, Ahsan H, Pierce BL. 2020. Genetic determinants of reduced arsenic metabolism efficiency in the 10q24.32 region are associated with reduced as3mt expression in multiple human tissue types. Toxicol Sci 176(2):382–395, PMID: 32433756, https://doi.org/10.1093/toxsci/kfaa075.

Chi L, Bian X, Gao B, Ru H, Tu P, Lu K. 2016. Sex-Specific effects of arsenic exposure on the trajectory and function of the gut microbiome. Chem Res Toxicol 29(6):949–951, PMID: 27268458, https://doi.org/10.1021/acs.chemrestox.6b00066.

Chi L, Lai Y, Tu P, Liu CW, Xue J, Ru H, et al. 2019. Lipid and cholesterol homeostasis after arsenic exposure and antibiotic treatment in mice: potential role of the microbiota. Environ Health Perspect 127(9):097002, PMID: 31532247, https://doi.org/10.1289/EHP4415.

Concha G, Vogler G, Lezcano D, Nermell B, Vahter M. 1998. Exposure to inorganic arsenic metabolites during early human development. Toxicol Sci 44(2):185–190, PMID: 9742656, https://doi.org/10.1093/toxsci/44.2.185.

Cullen WR, McBride BC, Manji H, Pickett AW, Reglinski J. 1989. The metabolism of methylarsine oxide and sulfide. Appl Organomet Chem 3(1):71–78, https://doi.org/10.1002/aoc.590030107.

D'Ippoliti D, Santelli E, De Sario M, Scortichini M, Davoli M, et al. 2015. Arsenic in drinking water and mortality for cancer and chronic diseases in central Italy, 1990–2010. PLoS ONE 10(9):e0138182, PMID: 26383851, https://doi.org/10.1371/journal.pone.0138182.

Fängström B, Moore S, Nermell B, Kuenstl L, Goessler W, Grandér M, et al. 2008. Breast-feeding protects against arsenic exposure in Bangladeshi infants. Environ Health Perspect 116(7):963–969, PMID: 18629322, https://doi.org/10.1289/ehp.11094.

Farzan SF, Karagas MR, Chen Y. 2013. In utero and early life arsenic exposure in relation to long-term health and disease. Toxicol Appl Pharmacol 272(2):384–390, PMID: 23859881, https://doi.org/10.1016/j.taap.2013.06.030.

FDA (U.S. Food and Drug Administration). 2005. *Guidance for Industry: Estimating the Maximum Safe Starting Dose in Initial Clinical Trials for Therapeutics in Adult Healthy Volunteers*. https://www.fda.gov/regulatory-information/search-fda-guidance-documents/estimating-maximum-safe-starting-dose-initial-clinical-trials-therapeutics-adult-healthy-volunteers [accessed 16 April 2021].

Garry MR, Santamaria AB, Williams AL, DeSesso JM. 2015. *In utero* arsenic exposure in mice and early life susceptibility to cancer. Regul Toxicol Pharmacol 73(1):378–390, PMID: 26239692, https://doi.org/10.1016/j.yrtph.2015.07.023.

Gomez D, Owens GK. 2012. Smooth muscle cell phenotypic switching in atherosclerosis. Cardiovasc Res 95(2):156–164, PMID: 22406749, https://doi.org/10.1093/cvr/cvs115.

Hall M, Gamble M, Slavkovich V, Liu X, Levy D, Cheng Z, et al. 2007. Determinants of arsenic metabolism: blood arsenic metabolites, plasma folate, cobalamin, and homocysteine concentrations in maternal–newborn pairs. Environ Health Perspect 115(10):1503–1509, PMID: 17938743, https://doi.org/10.1289/ehp.9906.

Hamadani J, Tofail F, Nermell B, Gardner R, Shiraji S, Bottai M, et al. 2011. Critical windows of exposure for arsenic-associated impairment of cognitive function in pre-school girls and boys: a population-based cohort study. Int J Epidemiol 40(6):1593–1604, PMID: 22158669, https://doi.org/10.1093/ije/dyr176.

Haseman JK, Kupper LL. 1979. Analysis of dichotomous response data from certain toxicological experiments. Biometrics 35(1):281–293, PMID: 574026, https://doi.org/10.2307/2529950.

Hoen AG, Madan JC, Li Z, Coker M, Lundgren SN, Morrison HG, et al. 2018. Sex-specific associations of infants' gut microbiome with arsenic exposure in a US population. Sci Rep 8(1):12627, PMID: 30135504, https://doi.org/10.1038/s41598-018-30581-9.

Howe CG, Niedzwiecki MM, Hall MN, Liu X, Ilievski V, Slavkovich V, et al. 2014. Folate and cobalamin modify associations between *S*-adenosylmethionine and methylated arsenic metabolites in arsenic-exposed Bangladeshi adults. J Nutr 144(5):690–697, PMID: 24598884, https://doi.org/10.3945/jn.113.188789.

Hsieh YC, Lien LM, Chung WT, Hsieh FI, Hsieh PF, Wu MM, et al. 2011. Significantly increased risk of carotid atherosclerosis with arsenic exposure and polymorphisms in arsenic metabolism genes. Environ Res 111(6):804–810, PMID: 21605854, https://doi.org/10.1016/j.envres.2011.05.003.

Islam MR, Attia J, Alauddin M, McEvoy M, McElduff P, Slater C, et al. 2014. Availability of arsenic in human milk in women and its correlation with arsenic

in urine of breastfed children living in arsenic contaminated areas in Bangladesh. Environ Health 13(1):101, PMID: 25471535, https://doi.org/10.1186/1476-069X-13-101.
James KA, Byers T, Hokanson JE, Meliker JR, Zerbe GO, Marshall JA. 2015. Association between lifetime exposure to inorganic arsenic in drinking water and coronary heart disease in Colorado residents. Environ Health Perspect 123(2):128–134, PMID: 25350952, https://doi.org/10.1289/ehp.1307839.
Jiang J, Liu M, Parvez F, Wang B, Wu F, Eunus M, et al. 2015. Association between arsenic exposure from drinking water and longitudinal change in blood pressure among HEALS cohort participants. Environ Health Perspect 123(8):806–812, PMID: 25816368, https://doi.org/10.1289/ehp.1409004.
Kile ML, Cardenas A, Rodrigues E, Mazumdar M, Dobson C, Golam M, et al. 2016. Estimating effects of arsenic exposure during pregnancy on perinatal outcomes in a Bangladeshi cohort. Epidemiology 27(2):173–181, PMID: 26583609, https://doi.org/10.1097/EDE.0000000000000416.
Kuo CC, Moon KA, Wang SL, Silbergeld E, Navas-Acien A. 2017. The association of arsenic metabolism with cancer, cardiovascular disease, and diabetes: a systematic review of the epidemiological evidence. Environ Health Perspect 125(8):087001, PMID: 28796632, https://doi.org/10.1289/EHP577.
Lazic SE, Essioux L. 2013. Improving basic and translational science by accounting for litter-to-litter variation in animal models. BMC Neurosci 14(1):37, PMID: 23522086, https://doi.org/10.1186/1471-2202-14-37.
Lemaire M, Lemarié CA, Flores Molina M, Guilbert C, Lehoux S, Mann KK. 2014. Genetic deletion of LXRα prevents arsenic-enhanced atherosclerosis, but not arsenic-altered plaque composition. Toxicol Sci 142(2):477–488, PMID: 25273567, https://doi.org/10.1093/toxsci/kfu197.
Lemaire M, Lemarié CA, Flores Molina M, Schiffrin EL, Lehoux S, Mann KK. 2011. Exposure to moderate arsenic concentrations increases atherosclerosis in ApoE$^{-/-}$ mouse model. Toxicol Sci 122(1):211–221, PMID: 21512104, https://doi.org/10.1093/toxsci/kfr097.
Lemaire M, Negro Silva LF, Lemarié CA, Bolt AM, Flores Molina M, Krohn RM, et al. 2015. Arsenic exposure increases monocyte adhesion to the vascular endothelium, a pro-atherogenic mechanism. PLoS One 10(9):e0136592, PMID: 26332580, https://doi.org/10.1371/journal.pone.0136592.
Libby P, Ridker PM, Hansson GK. 2011. Progress and challenges in translating the biology of atherosclerosis. Nature 473(7347):317–325, PMID: 21593864, https://doi.org/10.1038/nature10146.
Lindberg AL, Ekström EC, Nermell B, Rahman M, Lönnerdal B, Persson LA, et al. 2008. Gender and age differences in the metabolism of inorganic arsenic in a highly exposed population in Bangladesh. Environ Res 106(1):110–120, PMID: 17900557, https://doi.org/10.1016/j.envres.2007.08.011.
Makhani K, Chiavatti C, Plourde D, Negro Silva LF, Lemaire M, Lemarié CA, et al. 2018. Using the apolipoprotein E knock-out mouse model to define atherosclerotic plaque changes induced by low dose arsenic. Toxicol Sci 166(1):213–218, PMID: 30376133, https://doi.org/10.1093/toxsci/kfy201.
Mandal BK, Suzuki KT. 2002. Arsenic round the world: a review. Talanta 58(1):201–235, PMID: 18968746, https://doi.org/10.1016/S0039-9140(02)00268-0.
Mateen FJ, Grau-Perez M, Pollak JS, Moon KA, Howard BV, Umans JG, et al. 2017. Chronic arsenic exposure and risk of carotid artery disease: the Strong Heart Study. Environ Res 157:127–134, PMID: 28554006, https://doi.org/10.1016/j.envres.2017.05.020.
McLean RA, Sanders WL, Stroup WW. 1991. A unified approach to mixed linear models. Am Stat 45(1):54–64, https://doi.org/10.1080/00031305.1991.10475767.
Meza M, Gandolfi AJ, Klimecki WT. 2007. Developmental and genetic modulation of arsenic biotransformation: a gene by environment interaction? Toxicol Appl Pharmacol 222(3):381–387, PMID: 17306849, https://doi.org/10.1016/j.taap.2006.12.018.
Moon KA, Oberoi S, Barchowsky A, Chen Y, Guallar E, Nachman KE, et al. 2017. A dose-response meta-analysis of chronic arsenic exposure and incident cardiovascular disease. Int J Epidemiol 46(6):1924–1939, PMID: 29040626, https://doi.org/10.1093/ije/dyx202.
Naujokas MF, Anderson B, Ahsan H, Aposhian HV, Graziano JH, Thompson C, et al. 2013. The broad scope of health effects from chronic arsenic exposure: update on a worldwide public health problem. Environ Health Perspect 121(3):295–302, PMID: 23458756, https://doi.org/10.1289/ehp.1205875.
Navas-Acien A, Spratlen MJ, Abuawad A, Lolacono NJ, Bozack AK, Gamble MV. 2019. Early-life arsenic exposure, nutritional status, and adult diabetes risk. Curr Diab Rep 19(12):147, PMID: 31758285, https://doi.org/10.1007/s11892-019-1272-9.
Negro Silva LF, Lemaire M, Lemarié CA, Plourde D, Bolt AM, Chiavatti C, et al. 2017. Effects of inorganic arsenic, methylated arsenicals, and arsenobetaine on atherosclerosis in the mouse model and the role of As3MT-mediated methylation. Environ Health Perspect 125(7):077001, PMID: 28728140, https://doi.org/10.1289/EHP806.
Neilsen MG, Lombard PJ, Schalk LK. 2010. *Assessment of Arsenic Concentrations in Domestic Well Water, by Town, in Maine, 2005–09: U.S.* Geological Survey Scientific Investigations Report, 2010-5199. https://pubs.usgs.gov/sir/2010/5199/pdf/sir2010-5199_nielsen_arsenic_report_508.pdf [accessed 17 March 2021].
Nordstrom DK. 2002. Public health. Worldwide occurrences of arsenic in ground water. Science 296(5576):2143–2145, PMID: 12077387, https://doi.org/10.1126/science.1072375.
Osorio-Yáñez C, Ayllon-Vergara JC, Aguilar-Madrid G, Arreola-Mendoza L, Hernández-Castellanos E, Barrera-Hernández A, et al. 2013. Carotid intima-media thickness and plasma asymmetric dimethylarginine in Mexican children exposed to inorganic arsenic. Environ Health Perspect 121(9):1090–1096, PMID: 23757599, https://doi.org/10.1289/ehp.1205994.
Padovani AM, Flores Molina M, Mann KK. 2010. Inhibition of liver X receptor/retinoid X receptor-mediated transcription contributes to the proatherogenic effects of arsenic in macrophages in vitro. Arterioscler Thromb Vasc Biol 30(6):1228–1236, PMID: 20339114, https://doi.org/10.1161/ATVBAHA.110.205500.
Peng C, Xu X, Li Y, Li X, Yang X, Chen H, et al. 2020. Sex-specific association between the gut microbiome and high-fat diet-induced metabolic disorders in mice. Biol Sex Differ 11(1):5, PMID: 31959230, https://doi.org/10.1186/s13293-020-0281-3.
Pérez-Carrera A, Fernández Cirelli A. 2010. Arsenic and water quality challenges in South America. In: *Water and Sustainability in Arid Regions: an Interdisciplinary Exploration of Human and Environmental Interactions*. Schneier-Madanes G, Courel MF, eds. Dordrecht, Netherlands: Springer.
Petrick JS, Jagadish B, Mash EA, Aposhian HV. 2001. Monomethylarsonous acid (MMA^{III}) and arsenite: LD_{50} in hamsters and in vitro inhibition of pyruvate dehydrogenase. Chem Res Toxicol 14(6):651–656, PMID: 11409934, https://doi.org/10.1021/tx000264z.
Pierce BL, Kibriya MG, Tong L, Jasmine F, Argos M, Roy S, et al. 2012. Genome-wide association study identifies chromosome 10q24.32 variants associated with arsenic metabolism and toxicity phenotypes in Bangladesh. PLoS Genet 8(2):e1002522, PMID: 22383894, https://doi.org/10.1371/journal.pgen.1002522.
Pilsner JR, Liu X, Ahsan H, Ilievski V, Slavkovich V, Levy D, et al. 2009. Folate deficiency, hyperhomocysteinemia, low urinary creatinine, and hypomethylation of leukocyte DNA are risk factors for arsenic-induced skin lesions. Environ Health Perspect 117(2):254–260, PMID: 19270796, https://doi.org/10.1289/ehp.11872.
Pinheiro JC, Bates DM. 2000. *Mixed-Effects Models in S and S-PLUS*. New York, NY: Springer.
Rahman M, Sohel N, Yunus M, Chowdhury ME, Hore SK, Zaman K, et al. 2013. Increased childhood mortality and arsenic in drinking water in Matlab, Bangladesh: a population-based cohort study. PLoS One 8(1):e55014, PMID: 23383038, https://doi.org/10.1371/journal.pone.0055014.
Roh T, Lynch CF, Weyer P, Wang K, Kelly KM, Ludewig G. 2017. Low-level arsenic exposure from drinking water is associated with prostate cancer in Iowa. Environ Res 159:338–343, PMID: 28841521, https://doi.org/10.1016/j.envres.2017.08.026.
Roseboom TJ, van der Meulen JH, Osmond C, Barker DJ, Ravelli AC, Schroeder-Tanka JM, et al. 2000. Coronary heart disease after prenatal exposure to the Dutch famine, 1944–45. Heart 84(6):595–598, PMID: 11083734, https://doi.org/10.1136/heart.84.6.595.
Schläwicke Engström K, Broberg K, Concha G, Nermell B, Warholm M, Vahter M. 2007. Genetic polymorphisms influencing arsenic metabolism: evidence from Argentina. Environ Health Perspect 115(4):599–605, PMID: 17450230, https://doi.org/10.1289/ehp.9734.
Schneider CA, Rasband WS, Eliceiri KW. 2012. NIH image to ImageJ: 25 years of image analysis. Nat Methods 9(7):671–675, PMID: 22930834, https://doi.org/10.1038/nmeth.2089.
Simeonova PP, Hulderman T, Harki D, Luster MI. 2003. Arsenic exposure accelerates atherogenesis in apolipoprotein E$^{-/-}$ mice. Environ Health Perspect 111(14):1744–1748, PMID: 14594625, https://doi.org/10.1289/ehp.6332.
Smith AH, Marshall G, Liaw J, Yuan Y, Ferreccio C, Steinmaus C. 2012. Mortality in young adults following *in utero* and childhood exposure to arsenic in drinking water. Environ Health Perspect 120(11):1527–1531, PMID: 22949133, https://doi.org/10.1289/ehp.1104867.
Smith AH, Marshall G, Roh T, Ferreccio C, Liaw J, Steinmaus C. 2018. Lung, bladder, and kidney cancer mortality 40 years after arsenic exposure reduction. J Natl Cancer Inst 110(3):241–249, PMID: 29069505, https://doi.org/10.1093/jnci/djx201.
Smith DD, Tan X, Tawfik O, Milne G, Stechschulte DJ, Dileepan KN. 2010. Increased aortic atherosclerotic plaque development in female apolipoprotein E-null mice is associated with elevated thromboxane A2 and decreased prostacyclin production. J Physiol Pharmacol 61(3):309–316, PMID: 20610861.
Spratlen MJ, Grau-Perez M, Best LG, Yracheta J, Lazo M, Vaidya D, et al. 2018. The association of arsenic exposure and arsenic metabolism with the metabolic syndrome and its individual components: prospective evidence from the Strong Heart Family Study. Am J Epidemiol 187(8):1598–1612, PMID: 29554222, https://doi.org/10.1093/aje/kwy048.
Srivastava S, D'Souza SE, Sen U, States JC. 2007. *In utero* arsenic exposure induces early onset of atherosclerosis in ApoE$^{-/-}$ mice. Reprod Toxicol 23(3):449–456, PMID: 17317095, https://doi.org/10.1016/j.reprotox.2007.01.005.
Srivastava S, Vladykovskaya EN, Haberzettl P, Sithu SD, D'Souza SE, States JC. 2009. Arsenic exacerbates atherosclerotic lesion formation and inflammation

in ApoE-/- mice. Toxicol Appl Pharmacol 241(1):90–100, PMID: 19682479, https://doi.org/10.1016/j.taap.2009.08.004.
States JC, Singh AV, Knudsen TB, Rouchka EC, Ngalame NO, Arteel GE, et al. 2012. Prenatal arsenic exposure alters gene expression in the adult liver to a proinflammatory state contributing to accelerated atherosclerosis. PLoS One 7(6): e38713, PMID: 22719926, https://doi.org/10.1371/journal.pone.0038713.
Steinmaus C, Ferreccio C, Acevedo J, Balmes JR, Liaw J, Troncoso P, et al. 2016. High risks of lung disease associated with early-life and moderate lifetime arsenic exposure in northern Chile. Toxicol Appl Pharmacol 313:10–15, PMID: 27725189, https://doi.org/10.1016/j.taap.2016.10.006.
Stýblo M, Drobná Z, Jaspers I, Lin S, Thomas DJ. 2002. The role of biomethylation in toxicity and carcinogenicity of arsenic: a research update. Environ Health Perspect 110(suppl 5):767–771, PMID: 12426129, https://doi.org/10.1289/ehp.110-1241242.
Thomas DJ. 2007. Molecular processes in cellular arsenic metabolism. Toxicol Appl Pharmacol 222(3):365–373, PMID: 17397889, https://doi.org/10.1016/j.taap.2007.02.007.
Vahter M, Berglund M, Åkesson A, Lidén C. 2002. Metals and women's health. Environ Res 88(3):145–155, PMID: 12051792, https://doi.org/10.1006/enrs.2002.4338.
Waalkes MP, Ward JM, Liu J, Diwan BA. 2003. Transplacental carcinogenicity of inorganic arsenic in the drinking water: induction of hepatic, ovarian, pulmonary, and adrenal tumors in mice. Toxicol Appl Pharmacol 186(1):7–17, PMID: 12583988, https://doi.org/10.1016/S0041-008X(02)00022-4.
Wang CH, Chen CL, Hsiao CK, Chiang FT, Hsu LI, Chiou HY, et al. 2010. Arsenic-induced QT dispersion is associated with atherosclerotic diseases and predicts long-term cardiovascular mortality in subjects with previous exposure to arsenic: a 17-year follow-up study. Cardiovasc Toxicol 10(1):17–26, PMID: 19957052, https://doi.org/10.1007/s12012-009-9059-x.
Wang H, Li J, Zhang X, Zhu P, Hao JH, Tao FB, et al. 2018. Maternal serum arsenic level during pregnancy is positively associated with adverse pregnant outcomes in a Chinese population. Toxicol Appl Pharmacol 356:114–119, PMID: 30075163, https://doi.org/10.1016/j.taap.2018.07.030.
WHO (World Health Organization). 2008. Chapter 12. Chemical fact sheets. In: *Guidelines for Drinking-Water Quality [electronic resource]*. 3rd ed. Geneva, Switzerland: World Health Organization, 306–308b. https://www.who.int/water_sanitation_health/dwq/GDW12rev1and2.pdf?ua=1 [accessed 16 April 2021].
Winterbottom EF, Koestler DC, Fei DL, Wika E, Capobianco AJ, Marsit CJ, et al. 2017. The aquaglyceroporin AQP9 contributes to the sex-specific effects of *in utero* arsenic exposure on placental gene expression. Environ Health 16(1):59, PMID: 28615018, https://doi.org/10.1186/s12940-017-0267-8.
Xu L, Yokoyama K, Tian Y, Piao FY, Kitamura F, Kida H, et al. 2011. Decrease in birth weight and gestational age by arsenic among the newborn in Shanghai, China. Nihon Koshu Eisei Zasshi 58(2):89–95, PMID: 21473424.
Young JL, Cai L, States JC. 2018. Impact of prenatal arsenic exposure on chronic adult diseases. Syst Biol Reprod Med 64(6):469–483, PMID: 29873257, https://doi.org/10.1080/19396368.2018.1480076.
Yuan Y, Marshall G, Ferreccio C, Steinmaus C, Selvin S, Liaw J, et al. 2007. Acute myocardial infarction mortality in comparison with lung and bladder cancer mortality in arsenic-exposed region II of Chile from 1950 to 2000. Am J Epidemiol 166(12):1381–1391, PMID: 17875584, https://doi.org/10.1093/aje/kwm238.